NUREG/IA-0221


# International Agreement Report

# Reactor Trip Analysis at Krško Nuclear Power Plant

Prepared by:
A. Prošek, B. Mavko

Jožef Stefan Institute
Jamova cesta 39
SI-1000 Ljubljana, Slovenia

A. Calvo, NRC Project Manager

**Office of Nuclear Regulatory Research**
**U.S. Nuclear Regulatory Commission**
**Washington, DC 20555-0001**

**February 2010**

Prepared as part of
The Agreement on Research Participation and Technical Exchange
Under the Thermal-Hydraulic Code Applications and Maintenance Program (CAMP)

**Published by**
**U.S. Nuclear Regulatory Commission**

## AVAILABILITY OF REFERENCE MATERIALS IN NRC PUBLICATIONS

### NRC Reference Material

As of November 1999, you may electronically access NUREG-series publications and other NRC records at NRC's Public Electronic Reading Room at http://www.nrc.gov/reading-rm.html. Publicly released records include, to name a few, NUREG-series publications; *Federal Register* notices; applicant, licensee, and vendor documents and correspondence; NRC correspondence and internal memoranda; bulletins and information notices; inspection and investigative reports; licensee event reports; and Commission papers and their attachments.

NRC publications in the NUREG series, NRC regulations, and *Title 10, Energy*, in the *Code of Federal Regulations* may also be purchased from one of these two sources.

1. The Superintendent of Documents
   U.S. Government Printing Office
   Mail Stop SSOP
   Washington, DC 20402–0001
   Internet: bookstore.gpo.gov
   Telephone: 202-512-1800
   Fax: 202-512-2250
2. The National Technical Information Service
   Springfield, VA 22161–0002
   www.ntis.gov
   1–800–553–6847 or, locally, 703–605–6000

A single copy of each NRC draft report for comment is available free, to the extent of supply, upon written request as follows:

Address: Office of the Chief Information Officer,
Reproduction and Distribution
Services Section
U.S. Nuclear Regulatory Commission
Washington, DC 20555-0001
E-mail: DISTRIBUTION@nrc.gov
Facsimile: 301–415–2289

Some publications in the NUREG series that are posted at NRC's Web site address http://www.nrc.gov/reading-rm/doc-collections/nuregs are updated periodically and may differ from the last printed version. Although references to material found on a Web site bear the date the material was accessed, the material available on the date cited may subsequently be removed from the site.

### Non-NRC Reference Material

Documents available from public and special technical libraries include all open literature items, such as books, journal articles, and transactions, *Federal Register* notices, Federal and State legislation, and congressional reports. Such documents as theses, dissertations, foreign reports and translations, and non-NRC conference proceedings may be purchased from their sponsoring organization.

Copies of industry codes and standards used in a substantive manner in the NRC regulatory process are maintained at—

The NRC Technical Library
Two White Flint North
11545 Rockville Pike
Rockville, MD 20852–2738

These standards are available in the library for reference use by the public. Codes and standards are usually copyrighted and may be purchased from the originating organization or, if they are American National Standards, from—

American National Standards Institute
11 West 42nd Street
New York, NY 10036–8002
www.ansi.org
212–642–4900

Legally binding regulatory requirements are stated only in laws; NRC regulations; licenses, including technical specifications; or orders, not in NUREG-series publications. The views expressed in contractor-prepared publications in this series are not necessarily those of the NRC.

The NUREG series comprises (1) technical and administrative reports and books prepared by the staff (NUREG–XXXX) or agency contractors (NUREG/CR–XXXX), (2) proceedings of conferences (NUREG/CP–XXXX), (3) reports resulting from international agreements (NUREG/IA–XXXX), (4) brochures (NUREG/BR–XXXX), and (5) compilations of legal decisions and orders of the Commission and Atomic and Safety Licensing Boards and of Directors' decisions under Section 2.206 of NRC's regulations (NUREG–0750).

NUREG/IA-0221

# Reactor Trip Analysis at Krško Nuclear Power Plant

Manuscript Completed: July 2007
Date Published: January 2010

Prepared by: Andrej Prošek, Borut Mavko

Jožef Stefan Institute
Jamova cesta 39
SI-1000 Ljubljana, Slovenia

A. Calvo, NRC Project Manager

Prepared as part of
The Agreement on Research Participation and Technical Exchange
Under the Thermal-Hydraulic Code Applications and Maintenance Program (CAMP)

**Division**
**Office**
**U.S. Nuclear Regulatory Commission**
**Washington, DC 20555-0001**

# ABSTRACT

The reactor trip, which occurred at the Krško Nuclear Power Plant (NPP), on April 10, 2005, has been analyzed with the RELAP5/MOD3.3 Patch 03 computer code, the most current version released. The analysis was performed by the Jožef Stefan Institute, Reactor Engineering Division. The RELAP5 input model delivered by the Krško NPP was used. The purpose of the analysis was to evaluate the RELAP5 computer code against plant-measured data and validate the RELAP5 input model for the Krško NPP, which is a two-loop Westinghouse pressurized-water reactor. The event analyzed was a malfunction, which occurred during a power reduction sequence when regular, periodic testing of the turbine valves was performed. The malfunction led to a plant trip. All of the plant's safety systems responded according to the design specification, so the event caused no hazard to the environment or the plant staff and did not challenge the plant's safety. The RELAP5/MOD3.3 Patch 03 calculations agree very well with the plant-measured data, when operator actions are modeled properly. The analysis found that the long-term transient evolution is very sensitive to the steamflow after reactor trip. However, the calculation showed that the measured steamflow was larger than the calculated steam generated by available decay heat and therefore measurement of steamflow after reactor trip was not reliable. Therefore, the steamflow was tuned to obtain as good a match to the measured SG pressure as possible. The value of steamflow was physically reasonable but it is not known if this value reflects the reality of the transient.

# CONTENTS

## Figures

## Tables

# ACKNOWLEDGEMENT

The RELAP5/MOD3.3 Krško Nuclear Power Plant base input model and nodalization diagram are courtesy of the Krško Nuclear Power Plant.

# ABBREVIATIONS

| | |
|---|---|
| AFW | auxiliary feedwater |
| CVCS | chemical and volume control system |
| ECCS | emergency core cooling system |
| HPIS | high-pressure injection system |
| K | Kelvin |
| kg/s | kilogram per second |
| MFW | main feedwater |
| MPa | megapascal |
| MSIV | main steam isolation valve |
| MWt | megawatt thermal |
| NPP | nuclear power plant |
| NSSS | nuclear steam supply system |
| PORV | power-operated relief valve |
| PRZ | pressurizer |
| PWR | pressurized-water reactor |
| RCS | reactor coolant system |
| s | second |
| SI | safety injection |
| SG | steam generator |

# 1. INTRODUCTION

This report presents the analysis of an abnormal event that occurred at the Krško Nuclear Power Plant (NPP) on April 10, 2005. The purpose of the analysis, performed by Jožef Stefan Institute, Reactor Engineering Division, was to evaluate the RELAP5/MOD3.3 Patch 03 computer code (Ref. 1) against plant-measured data and validate the input model for the Krško NPP, which is a two-loop Westinghouse pressurized-water reactor (PWR). The analysis used the RELAP5 input model delivered by Krško NPP. This is a full two-loop plant model, which includes the major components of the primary and secondary system. The model delivered by Krško NPP had two limitations: (1) the secondary side was only modeled up to the turbine and (2) auxiliary systems consuming steam after a transient were not included. These limitations are significant because steamflow is very important to the behavior of the secondary pressure in terms of its influence on the primary pressure. Both pressures dictate the operation of the control and safety systems. The analysis was performed for uprated power conditions (2,000 megawatt thermal (MWt)) ($6{,}824 \cdot 10^6$ Btu/hr) with new steam generators (SGs) and Cycle 21 settings, which corresponded to the plant state after outage and refueling in September 2004.

A malfunction occurred during a power reduction sequence when regular, periodic testing of the turbine valves was performed. This malfunction led to a plant trip. All of the plant's safety systems responded according to the design specification, so the event caused no hazard to the environment or plant staff and did not challenge the plant safety. The scope of the analysis was to evaluate the transient and to compare the measured data to the calculations, as well as to simulate the testing of the governor valves, which involved a power reduction from 100 percent to below 92 percent.

The analysis was divided into five phases. The first phase demonstrated the steady-state condition at 100-percent power. In the second phase, the power was reduced from 100 percent to 91.72 percent. The third phase simulated one cycle of the turbine governor valve closing and opening in order to recreate, as closely as possible, the initial conditions of the transient. In Phase 4, the steady state at a power level of 91.72 percent was verified by comparing calculated initial conditions with plant data, which were available for 53 seconds before the transient started. Finally, in the last phase, the transient was analyzed using data collected for a period of 1,825 seconds after the transient began. Measurement data beyond this timeframe were not available.

Section 2 briefly describes the Krško NPP, and Section 3 describes the RELAP5 input model. Section 4 details the modeled scenario. Section 5 presents the results of the analysis, and compares the RELAP5 data to the plant-measured data. Section 6 summarizes the run statistics, and Section 7 provides the conclusions of the analysis.

# 2. PLANT DESCRIPTION

The Krško NPP is a Westinghouse 2-loop PWR plant with a large dry containment. The plant has been in commercial operation since 1983. After the plant was modernized in 2000, the plant fuel cycle was gradually lengthened from 12 (Cycle 17) to 18 months (Cycle 21).

The Krško NPP nuclear steam supply system (NSSS) has a power rating of 2,000 MWt ($6{,}824 \cdot 10^6$ Btu/hr) (1,882 MWt ($6{,}422 \cdot 10^6$ Btu/hr) before modernization and power uprate), comprising a core output of 1,994 MWt ($6{,}804 \cdot 10^6$ Btu/hr) (1,876 MWT ($6{,}401 \cdot 10^6$ Btu/hr)) before modernization and power uprate) plus a reactor coolant pump heat input of 6 MWt ($205 \cdot 10^6$ Btu/hr). The NSSS consists of a PWR, reactor coolant system (RCS), and associated auxiliary fluid systems. The RCS is arranged as two closed reactor coolant loops connected in parallel to the reactor vessel, each containing a reactor coolant pump and an SG. An electrically heated pressurizer (PRZ) is connected to one of the loops.

The reactor core is composed of 121 fuel assemblies. Square spacer grid assemblies and the upper and lower end fitting assemblies support the fuel rods in fuel assemblies. Each fuel assembly is composed of 16 x 16 rods; of these, only 235 places are used by fuel rods. Of the 21 remaining places, 20 are provided with thimble tubes, which may be reserved for control rods. These 20 places are evenly and symmetrically distributed across the cross section of the assembly. The last remaining place is provided for the control instrumentation tube for the in-core thimble.

The reactor coolant pumps, one per coolant loop, are Westinghouse vertical, single-stage centrifugal pumps of the shaft-seal type.

The SGs, one per loop, are vertical U-tube unit, Siemens-Framatome type SG 72 W/D4-2 SGs, which were installed during the plant modernization in 2000. These SGs replaced the highly degraded Westinghouse D-4 SGs, each having preheating section.

The plant includes the following engineered safety features to prevent accident propagation or to limit the consequences of postulated accidents, which might otherwise lead to system damage and release of fission products:

- containment spray system
- hydrogen control system
- emergency core cooling system (ECCS)
- component cooling water system
- essential service water system
- auxiliary feedwater (AFW) system

In 2006, the main turbine was replaced to gain additional power from the new SGs. Note that the event took place in 2005; therefore, the model did not reflect the replacement of the main turbine.

# 3. INPUT MODEL DESCRIPTION

To perform this analysis, the Krško NPP provided the base RELAP5 input model, referred to as the "master input deck," which has been used for several analyses, including reference calculations for Krško full-scope simulator verification (Refs. 2, 3, 4). Figure 1 presents the scheme of the Krško NPP nodalization for the RELAP5/MOD3.3 code. The analysis used a full two-loop plant model provided by Krško NPP. The model includes the new Siemens-Framatome type SG 72 W/D4-2 replacement SGs. The analysis was performed for uprated power conditions (2,000 MWt ($6{,}824 \cdot 10^6$ Btu/hr)) with new SGs and Cycle 21 settings, corresponding to the plant state after outage and refueling in September 2004.

The model consists of 469 control volumes, 497 junctions, and 378 heat structures with 2,107 radial mesh points. In addition, 574 control variables and 405 logical conditions (trips) represent the instrumentation, regulation isolation, safety injection (SI) and AFW triggering logic, and steamline isolation.

## 3.1 Hydrodynamic Component Description

Components numbered from 101 to 165 represent the reactor vessel as follows:

| | |
|---|---|
| 171, 173, and 175 | lower downcomer |
| 101 and 103 | lower head |
| 105 | lower plenum |
| 107 | core inlet |
| 111 | reactor core |
| 115 | core baffle bypass |
| 121 | core outlet |
| 125, 131, and 141 | upper plenum |
| 151 and 153 | upper head |
| 165 | upper downcomer |
| 113 and 145 | guide tubes |

Components 51, 53, and 55 represent the PRZ surge line, and volumes 61, 63, 65, 67, and 69 represent the PRZ vessel. PRZ spray lines (80, 81, and 84) are connected to the top of the PRZ vessel and include spray valves 82 and 83. Valves 28 and 32 represent the two PRZ power-operated relief valves (PORVs), and valves 14 and 22 represent PRZ safety valves.

The following components represent the primary piping:

| | |
|---|---|
| 201, 203, 205, 207, 209, and 211 | hot leg no.1 |
| 251, 253, 255, 257, and 259 | intermediate leg no.1 with cold leg no.1 loop seal |
| 265, 271, 273, 275, 277, and 279 | cold leg no.1 with the primary coolant pump no.1 |
| 301, 303, 305, 307, 309, and 311 | hot leg no.2 |
| 351, 353, 355, 357, and 359 | intermediate leg no.2 with cold leg no.2 loop seal |
| 365, 371, 373, 375, 377, and 379 | cold leg no.2 with the primary coolant pump no.2 |

Loops are symmetrical except for the PRZ surge line and chemical and volume control system (CVCS) connections layout.

The piping nodalization and connections of the ECCS are represented by hydrodynamic components numbered from 701 to 882. The hydrodynamic components representing the high-pressure injection system (HPIS) pumps are time-dependent junctions 703 and 803, while time-dependent junctions 750 and 850 represent the low-pressure injection system pumps. Accumulators are numbered 701 and 801; their lineup provides cold-leg injection only. The ECCS connects to both cold legs (junctions 719-01 and 819-01). Direct vessel ECCS injection through junctions 746 and 748 opens simultaneously upon SI signal generation.

The primary side of the SG is represented by inlet and outlet plenum, with a single pipe representing the U-tube bundle:

| | |
|---|---|
| 215, 217, and 219 | SG 1 inlet plenum (hot side) and tubesheet inlet |
| 223, 225, 227, 233, 235, and 237 | SG 1 U-tubes |
| 241, 243, and 245 | SG 1 tubesheet outlet and outlet plenum (cold side) |
| 315, 317, and 319 - | SG 2 inlet plenum (hot side) and tubesheet inlet |
| 323, 325, 327, 333, 335, and 337 | SG 2 U-tubes |
| 341, 343, and 345 | SG 2 tubesheet outlet and outlet plenum (cold side) |

The following hydrodynamic components represent the parts of the SG secondary side:

| | |
|---|---|
| 415, 417, and 419 | SG 1 riser |
| 421 and 427 | SG 1 separator and separator pool |
| 411 and 413 | SG 1 downcomer |
| 423, 425, and 429 | SG 1 steam dome |
| 515, 517, and 519 | SG 2 riser |
| 521 and 527 | SG 2 separator and separator pool |
| 511 and 513 | SG 2 downcomer |
| 523, 525, and 529 | SG 2 steam dome |

Main steamlines are represented by volumes 451, 453, 455, 457, 459, and 461 (SG 1) and 551, 553, 555, 557, 559, and 561 (SG 2), divided by main steam isolation valves (MSIVs) (458 and 558). SG relief (482 and 582) and safety valves (484, 486, 488, 492, 494, 584, 586, 588, 592, and 594) are situated upstream of the isolation valves. Turbine valve (604) and steam dump (611) flow is regulated by corresponding logic.

Main feedwater (MFW) piping is represented by volumes 471, 473, 475, 407, 409 (SG 1) and 571, 573, 575, 507, and 509 (SG 2), branching from the MFW header (500).

AFW injects above the SG riser (for SG 1 via volumes 437, 443, 445, and 447; for SG 2 via volumes 537, 543, 545, and 547) and its piping is represented by volumes 671 and 673 (motor-driven AFW 1); 675 and 677 (motor-driven AFW 2); and 681, 683, 685, 687, 695, and 697 (turbine-driven AFW).

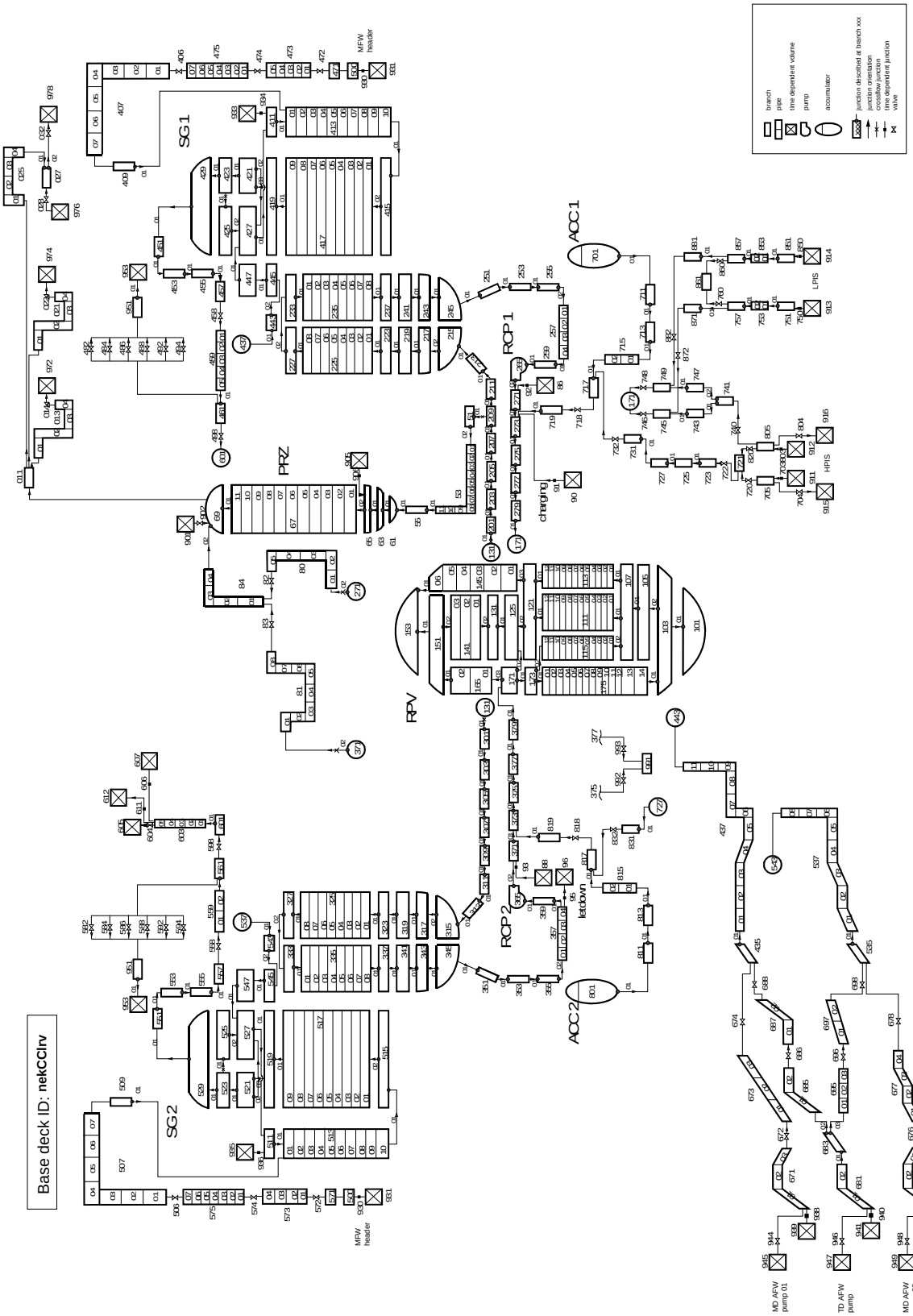


**Figure 1 Krško NPP nodalization scheme**

## 3.2 Regulation and Protection Logic

To accurately represent the behavior of the Krško NPP, the model includes a considerable number of control variables and general tables. They represent protection, monitoring, and simplified control systems used only during steady-state initialization, as well as the following main plant control systems:

- rod control system
- PRZ pressure control system
- PRZ level control system
- SG level control system
- steam dump

It must be noted that the rod control system has been modeled for point kinetics. The present model can be used for transient analysis with either of the following two options:

(1) constant or predefined core power transient as a function of time (including decay power calculation)

(2) rod control system in auto or manual mode

The following plant protection systems are defined using trip logic:

- reactor trip
- SI signal
- turbine trip
- steamline isolation
- MFW isolation
- AFW start

# 4. ABNORMAL EVENT DESCRIPTION

The Krško NPP technical specifications required that the operability of the turbine overspeed protection system be demonstrated at least once every 31 days by cycling each of the high-pressure turbine governor and stop valves through at least one complete cycle from the running position. The test procedure consists of two steps. In the first step, the turbine (and thus the reactor power) must be reduced below 92 percent to fulfill test conditions. In the second step, the test of the turbine governor and stop valves is performed.

In the first step, the turbine power is reduced until governor valve no. 4 is closed. The turbine power is then reduced by another 7 percent until the nuclear power is less than or equal to 92 percent. The closure of the governor valves is then changed from sequential to single mode of operation. The position of the governor valves is checked to ensure that it is less than or equal to 35 percent of opening. If it is larger, the power should be reduced before the test start.

In the second step of the turbine valves test, the allowed maximum position of the governor valves is defined as 55 percent of opening. To fulfill this condition, the button “valve position limit display” is pushed to read “flow demand” and “valve position limit.” The valve position limit is then raised to 160 percent and the valves are tested one by one. The valve is first closed and then opened to its initial value. When all valves are tested, the valve position limit is decreased to the value at test start (i.e., less than or equal to 35 percent of opening). When lowering the valve position limit, the value should stay above the flow demand value. If not, the governor valves start to close. This is what happened during the April 5, 2005, transient. The valves closed for 5 seconds, from the 35.5-percent to the 12.2-percent position. The valves then stabilized for 12 seconds, during which time the position began to increase to 14 percent, followed by full closure. The valve positions indicate that the operator set the valve position limit below the flow demand; after 16 seconds, he attempted to restore the turbine flow. This resulted in a reactor trip, which occurred within the next 2 seconds or less (data were available in 2-second increments).

When considering the measured data for the governor valve position at 12.2 percent, it appears that the operator confused the desired value of the governor valve position (less than or equal to 35 percent opening) with the valve position limit. In other words, the governor valve position value of 12.2 percent is equal to 0.35 times 34.9 percent, suggesting that at test start the governor valve position was 34.9 percent (less than or equal to 35 percent of opening) and the valve position limit was around 100 percent. This was the first operator error. When the operator noticed the decreased electrical power output, he attempted to correct the setpoint to the desired (i.e., higher) value, but he was not aware that the steam dump was operating. The increased demand for steamflow resulted in a high steamflow, which caused a pressure drop. The low steamline pressure generated an SI signal. The SI signal led to the reactor trip signal, followed by the turbine trip. The SI signal also started both AFW pumps with a 25-second delay.

Measured data were available for a total of 1,878 seconds in 2-second increments. The data for the first 52 seconds represent the steady-state condition. At the 54-second mark, the governing valves were already closing, indicating that the transient started. Therefore, the governor valves were estimated to have started to close at 53 seconds, which is considered the transient start time (t = 0). The remaining data—up to 1,878 seconds—represent the transient, which lasted a total of 1,825 seconds.

# 5. RESULTS

The RELAP5/MOD3.3 P03 analysis was divided into two parts. In the first part, the activities in the plant before the transient were simulated because measured data were not available. This included the monthly testing of the turbine governor and stop valves. The purpose of this simulation was to recreate the steady-state condition before the reactor trip. As shown in Table 1, this part of the analysis consisted of four phases. The first phase demonstrated the steady state at a 100-percent power level. In the second phase, the power was reduced from 100 percent to 91.72 percent, and the steady state at a reduced power level was observed. The third phase simulated one cycle of turbine governor valve closing and opening in order to model the initial plant conditions as closely as possible. Although there are four turbine governor valves, the analysis was performed for only one governor valve because the procedure would be the same for each of the four governor valves. The analysis did not simulate the stop valves because they close when the governor control valve is fully closed. When the governor valve starts to open, the stop valves open as well. Phase 3 also demonstrated the steady state. At t = −500 seconds, the time-dependent junction component was replaced by the valve component, which caused some transient in the steamflow. Therefore, in Phase 4, steady-state calculations, which included the valve component, were performed at a power level of 91.72 percent. Phase 4 represented a slightly different plant condition because of the replaced time-dependent junction. This steady state was compared to the plant data, which were available for the 53 seconds before the transient began. The simulation in Part 1 eliminated the need to use artificial controls to achieve the steady-state condition at a power level of 91.72 percent.

The second part of the analysis, which was Phase 5, simulated the transient leading to the reactor trip, as well as the plant response to the turbine and reactor trip. The analysis denoted t = 0 seconds as the transient start time. Thus, Part 1 of the analysis encompassed the time period from t = –4,000 to t = 0 seconds. Part 2 of the analysis, in which the transient was evaluated, spanned the time period from t = 0 seconds to t = 1,900 seconds.

**Table 1 Phases of the Analysis**

| Phase of Analysis | Description of Phase and Analysis Duration |
|---|---|
| Phase 1 | Steady state at 100% power (1,000 s) |
| Phase 2 | Power reduction from 100% to 91.72% for valve testing (1,000 s) |
| Phase 3 | Cycling of one turbine governor valve (1,500 s) |
| Phase 4 | Steady state at 91.72% power (500 s) |
| Phase 5 | Turbine governor valve closure with reactor trip (1,900 s)* |

* Measured data were available for 1,825 seconds.

## 5.1 Part 1 of the Analysis—Testing of the Turbine Governor Valve

Phases 1 and 4 were steady-state calculations. Phases 2 and 3 were also simulated until the point at which steady state was achieved. The Phase 1 simulation was performed to verify steady state at 100 percent power, and the Phase 4 simulation was performed to verify steady state before the abnormal event began. The Phase 4 steady-state calculation was needed because the time-dependent junction component was replaced by the valve component. Only 53 seconds (from t = –53 seconds to t = 0 seconds) of measured steady-state data were

available. Based on the average of the sample data, the nuclear power level was at 91.72 percent. The analysis did not include a simple power reduction scheme to reduce power from 100 percent to 91.72 percent because, after being reduced below 92 percent, the reactor power level was decreasing and increasing as the turbine governor valves were cycling closed and open. To simulate the initial conditions as closely as possible, the model assumed that the power was reduced to 68.79 percent and then returned to 91.72 percent.

If the power level is reduced to 91.72 percent by inserting rods due to a power mismatch between the reactor power and turbine power, then the initial conditions will differ from the initial conditions created by withdrawing rods. This difference results from the deadband in the temperature error signal (i.e., the deadband between the reference temperature and the auctioneered average RCS temperature). The difference between the temperature at which the rods stop to move in and when they start to move out is 1.4 Kelvin (K) (2.5 degrees Fahrenheit). Such a difference causes a change in the pressure on the secondary side (a temperature change of 1 K corresponds to a pressure change of 0.125 megapascal (MPa) (18.1 psi)). To achieve as close to a match of the secondary-side pressure as possible, the analysis assumed that the last request was to withdraw the rods (in the test, the governor valve was first closed and then opened). Opening of the governing valves resulted in an increase in turbine power, and led to rod withdrawal. The initial secondary pressure is very important because the transient occurred on the secondary side, and the SI signal was actuated based on low steamline pressure.

Table 2 presents the initial plant conditions. The first two columns describe the plant variables and their units. The third column identifies the average value of the plant-measured initial condition. The data were averaged over the time interval between t = −53 seconds and t = 0 seconds because the measured values were oscillating slightly for some variables. The value t = 0 seconds signifies the start of the reactor trip transient. The fourth column provides the plant-measured initial conditions for this time, which differ from the average steady-state values in some cases. Finally, the last three columns list the steady-state values at the end of Phases 2, 3, and 4. The fifth column reports the calculated initial conditions after the initial power was reduced to below 92 percent (rod insertion at t = –2,000 seconds); the sixth column reports initial conditions after the rods were withdrawn (t = –500 seconds). Finally, the last column presents the initial conditions at the time the transient began (t = 0 seconds).

Note that, for power reduction, the RELAP5 component, TMDPJUN, was used to model turbine flow; therefore, another steady state was calculated when the TMDPJUN component was replaced by the valve component, which represented the turbine governor valves. In other words, the simulation of both Phase 2 (power reduction) and Phase 3 (governor valve testing) was extended until a steady state was reached.

**Table 2 Initial Conditions for Reactor Trip Transient**

| Variables | Unit | measured (average) | measured (t=0 s) | calculated (t=-2,000 s) | calculated (t=-500 s) | calculated (t=0 s) |
|---|---|---|---|---|---|---|
| PRZ pressure | MPa (psia) | 15.48 (2245) | 15.48 (2245) | 15.52 (2251) | 15.51 (2250) | 15.52 (2251) |
| SG 1 pressure | MPa (psia) | 6.42 (931) | 6.42 (931) | 6.59 (956) | 6.43 (933) | 6.47 (938) |
| SG 2 pressure | MPa (psia) | 6.40 (928) | 6.40 (928) | 6.57 (953) | 6.42 (931) | 6.45 (935) |
| Feedwater 1 mass flow rate | kg/s (lb/s) | 499.00 (1100.30) | 504.00 (1111.32) | 495.20 (1091.92) | 495.40 (1092.36) | 495.50 (1092.58) |
| Feedwater 2 mass flow rate | kg/s (lb/s) | 503.60 (1110.44) | 500.60 (1103.82) | 497.70 (1097.43) | 498.10 (1098.31) | 498.10 (1098.31) |
| Main steamline 1 mass flow rate | kg/s (lb/s) | 493.90 (1089.05) | 492.60 (1086.18) | 495.20 (1091.92) | 495.40 (1092.36) | 495.40 (1092.36) |
| Main steamline 2 mass flow rate | kg/s (lb/s) | 501.60 (1106.03) | 501.50 (1105.81) | 497.80 (1097.65) | 498.10 (1098.31) | 498.10 (1098.31) |
| PRZ liquid level | % | 53.02 | 52.95 | 56.10 | 51.88 | 52.63 |
| SG 1 narrow range level | % | 69.25 | 69.15 | 69.34 | 69.26 | 69.28 |
| SG 2 narrow range level | % | 69.06 | 69.40 | 69.34 | 69.25 | 69.28 |
| Nuclear power | % | 91.72 | 91.94 | 91.63 | 91.78 | 91.77 |
| Cold leg 1 temperature | K (˚F) | 559.41 (547.27) | 559.36 (547.18) | 560.74 (549.66) | 559.15 (546.80) | 559.51 (547.45) |
| Cold leg 2 temperature | K (˚F) | 559.57 (547.56) | 559.53 (547.48) | 560.59 (549.39) | 558.99 (546.51) | 559.35 (547.16) |
| Hot leg 1 temperature | K (˚F) | 593.92 (609.39) | 593.73 (609.04) | 594.64 (610.68) | 593.23 (608.14) | 593.55 (608.72) |
| Hot leg 2 temperature | K (˚F) | 594.58 (610.57) | 594.62 (610.65) | 594.64 (610.68) | 593.23 (608.14) | 593.55 (608.72) |
| Average RCS 1 temperature | K (˚F) | 576.63 (578.26) | 576.52 578.07) | 577.69 (580.17) | 576.19 (577.47) | 576.53 (578.08) |
| Average RCS 2 temperature | K (˚F) | 577.05 (579.02) | 577.05 (579.02) | 577.62 (580.05) | 576.11 (577.33) | 576.45 (577.94) |
| Programmed Tavg | K (˚F) | 576.90 (578.75) | 576.90 (578.75) | 576.97 (578.88) | 576.97 (578.88) | 577.00 (578.93) |

Figures 2 through 21 illustrate the main variables for the governor valve monthly testing and explain how the initial condition at a 91.72-percent power level was obtained. Where plant-measured data were available, the calculated and measured data were compared. The calculated data (labeled “cal”) were available for the time interval between t = −4000 seconds and t = 0 seconds, while the measured steady-state data were available for the time interval between t = −53 seconds to t = 0 seconds, for most of the important variables shown in Figures 2 through 21. Table 3 describes the variable identification used in the figures. The power reduction scheme was such that flow was reduced from a nominal value of 1,086 kilograms per second (kg/s) (2394 lb/s) to 991 kg/s (2185 lb/s), thereby simulating the initial test conditions. A test of the governor valve closing and opening was then performed (with flow decreasing to 743.25 kg/s (1638.59 lb/s) and then returning to 991 kg/s (2185 lb/s)). For

simplicity, the analysis simulated only one out of four valve testing cycles (closing and opening).

Because there were no measured data on the timing of valve closing and opening, the analysis assumed a 5 percent per minute load reduction and increase, as shown in Figure 4. In other words, 5 minutes were needed to achieve a 25-percent power reduction from the 91.72-percent power level, and 5 minutes were needed for the power to increase. In this way, the steam dump operation was prevented. Figure 4 indicates that the turbine flow was reduced linearly both during power reduction and valve cycling. At t = –500 seconds, the valve component was introduced, temporarily causing the flow to spike. Because the turbine is not modeled explicitly, but rather by logic, turbine power (Figure 5) is calculated as a function of flow (Figure 4). The control rods start to move in when the turbine flow demand is reduced and to move out when the turbine flow demand is increased (Figure 3). Rod movement causes the reactor power to change, as shown in Figure 2. Reference temperature follows the generated power (Figure 11). The PRZ level (Figure 13) shows a slight increase initially after power reduction (from t = −3,000 seconds to t = −2,880 seconds) as a result of the power imbalance. Rod motion and reactor power then decrease the RCS average temperature. The resulting density change brings the pressurizer level down at t = –2,400 seconds. During testing, the same phenomenon occurs when the governor valve closes. When the governor valve opens, the opposite phenomenon occurs.

Charging flow (Figure 14) also varies slightly to accommodate the density changes, and letdown flow (Figure 15) is held constant. Both flows are higher than the initial plant values. However, the difference between the flows is similar, and the letdown flow is higher than the charging flow in both the calculations and the plant measurements. The RCS average temperature does not decrease as expected in the initial 150 seconds of Phase 2 (until t = –2,850 seconds) because of a delay resulting from a combination of the loop transport time, resistance temperature detector manifold arrangement, and instrument processing time (Figure 10). The temperature then begins to decrease. At the beginning of Phase 3, similar to the above-described delay, the temperature first increases and then decreases. The temperature also starts to increase, with a delay, at t = –1,530 seconds (the turbine governor valve starts to open at t = –1,700 seconds).

Figures 6 through 9 represent the hot- and cold-leg temperatures. The differences between the measured and calculated initial values at t = 0 seconds were less than 0.4 K (0.72 ˚F), except for the hot leg 1 temperature. The reason for this exception is the nearly symmetrical conditions in the RELAP5 calculation; in the measured data, there is slight asymmetry between the steamflows and the hot-leg temperatures. The plant data seem consistent—the loop 2 hot-leg temperature is lower and the steamflow is higher. The initial SG 1 and 2 pressure overshoot (as depicted in Figures 16 and 17) in the beginning of Phase 2 is caused by the RCS average temperature. Continued rod motion (rod insertion) eventually brought the RCS average temperature to the reference temperature at around t = −2,400 seconds (i.e., the upper side of the deadband). When the turbine governor valve is tested, the SG pressure behaves similarly during valve closing, while opening the turbine governor valves initially caused a further decrease in pressure. Finally, rod withdrawal brought the RCS temperature to the reference temperature, thereby increasing both SG pressures (from t = −1,370 seconds to t = −1,170 seconds).

As rods stop to move out (at the lower side of the deadband), the SG pressure differs from the pressure before valve testing despite the approximately same reactor power level. When the valve component was introduced into the input model, the SG pressure first spiked and then stabilized in Phase 4 at a slightly higher value than at the end of Phase 3. The steamflow

(Figures 18 and 19) follows the modeled turbine flow. At the end of Phase 4, the calculated steamflows are in good agreement with the steady-state steamflows measured at the plant. The feed flow/steamflow mismatch circuit in the SG level control regulates the feedwater flow (Figure 20 and Figure 21). Again, the calculated feedwater flows agree well with the steady-state feedwater flows measured at the plant.

**Table 3 Variables Identification in Figures**

| ID | Code | Variable |
|---|---|---|
| 1 | AF00793_FT205 | Charging flow |
| 2 | AF00795_FT132 | Letdown flow |
| 3 | AF00798_FT510A | Feedwater flow SG 1 |
| 4 | AF00799_FT512A | Steamflow SG 1 |
| 5 | AF00803_FT520A | Feedwater flow SG 2 |
| 6 | AF00804_FT522A | Steamflow SG 2 |
| 7 | AF03308_FT302 | AFW 1 volumetric flow |
| 8 | AF03309_FT301 | AFW 1 volumetric flow |
| 9 | AF04033_FT901 | SI 1 volumetric flow |
| 10 | AF04034_FT902 | SI 2 volumetric flow |
| 11 | AL00813_LT517 | SG 1 narrow range level |
| 12 | AL00815_LT527 | SG 2 narrow range level |
| 13 | AL00818_LT465 | PRZ level |
| 14 | AN00846_NM41F | Core power |
| 15 | AP00871_PT514 | SG 1 pressure |
| 16 | AP00872_PT524 | SG 2 pressure |
| 17 | AP00874_PT455 | PRZ pressure |
| 18 | AT00941_TE412A | RCS average temperature |
| 19 | AT00942_TE410B | Cold leg loop 1 temperature |
| 20 | AT01360_TE420B | Cold leg loop 2 temperature |
| 21 | AT01377_TE660 | Reference (programmed) temperature |
| 22 | AT05973_TE410A | Hot leg loop 1 temperature |
| 23 | AT05974_TE420A | Hot leg loop 2 temperature |

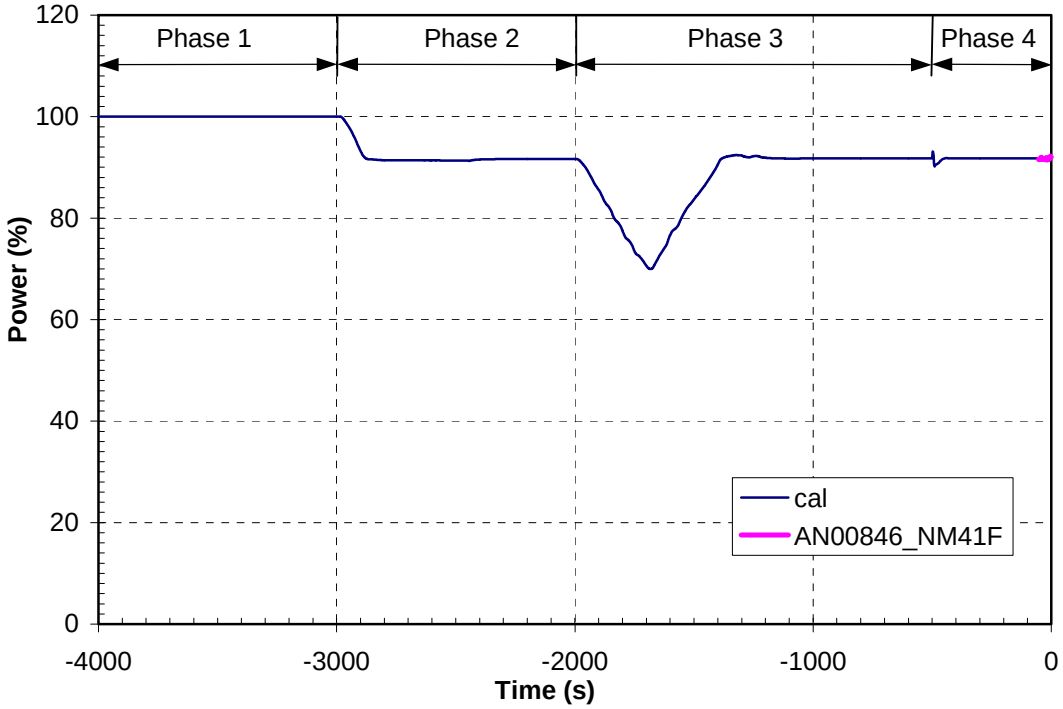


**Figure 2 Core power—testing of turbine governor valve**

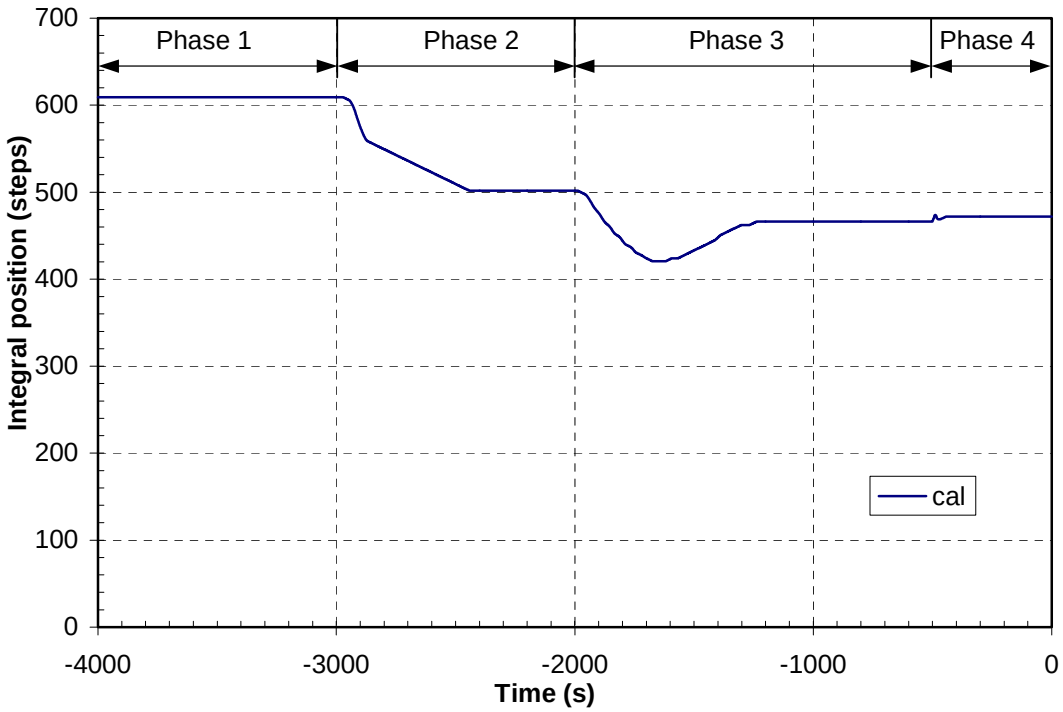


**Figure 3 Rod position—testing of turbine governor valve**

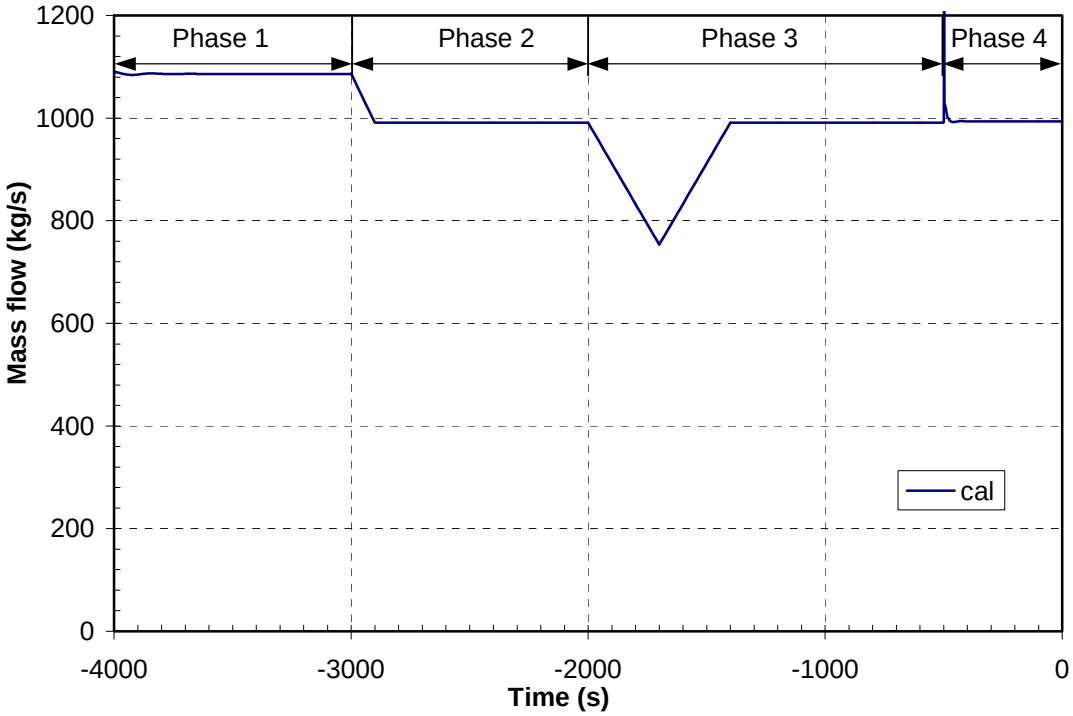


**Figure 4 Turbine flow—testing of turbine governor valve**

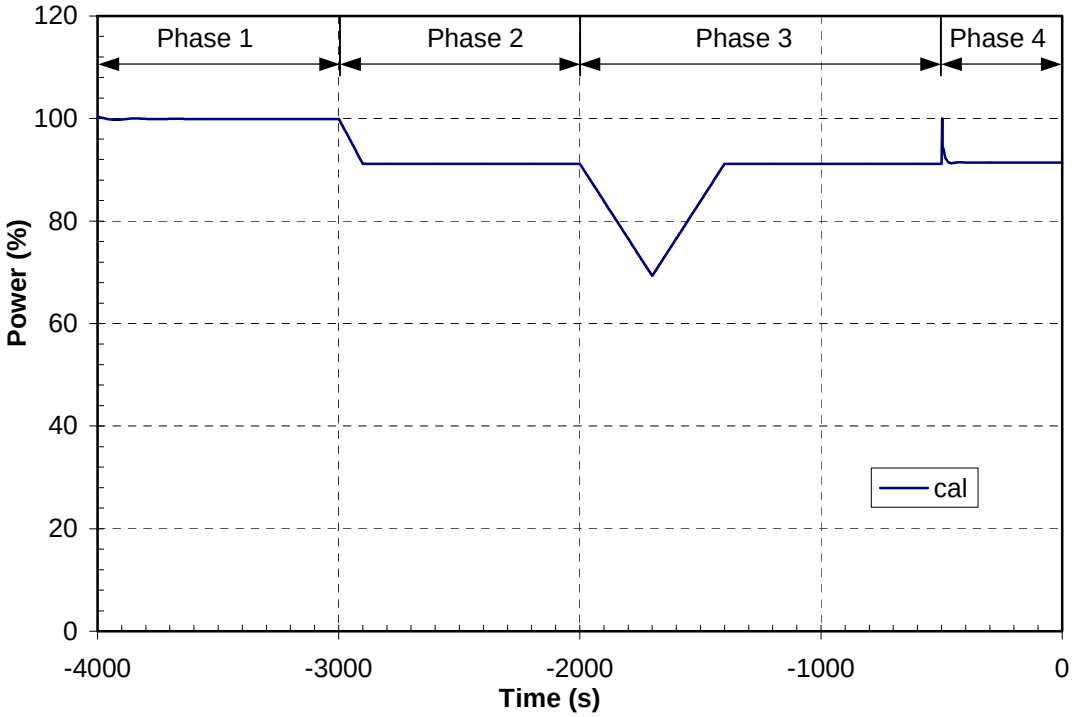


**Figure 5 Turbine power—testing of turbine governor valve**

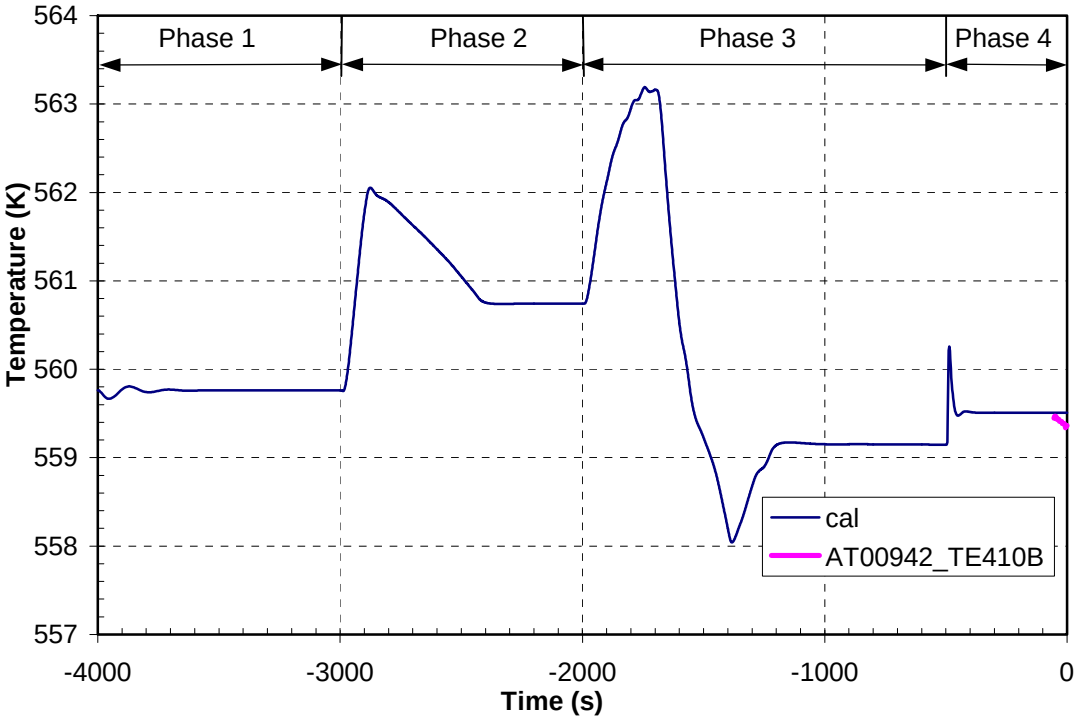


**Figure 6 Cold leg loop 1 temperature—testing of turbine governor valve**

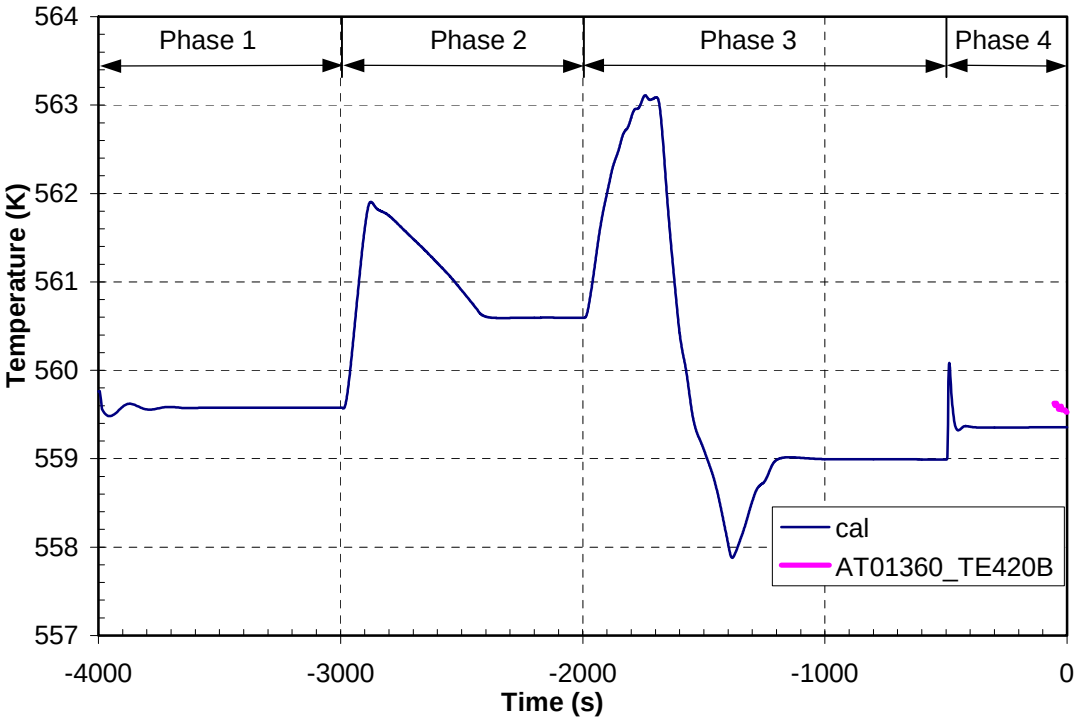


**Figure 7 Cold leg loop 2 temperature—testing of turbine governor valve**

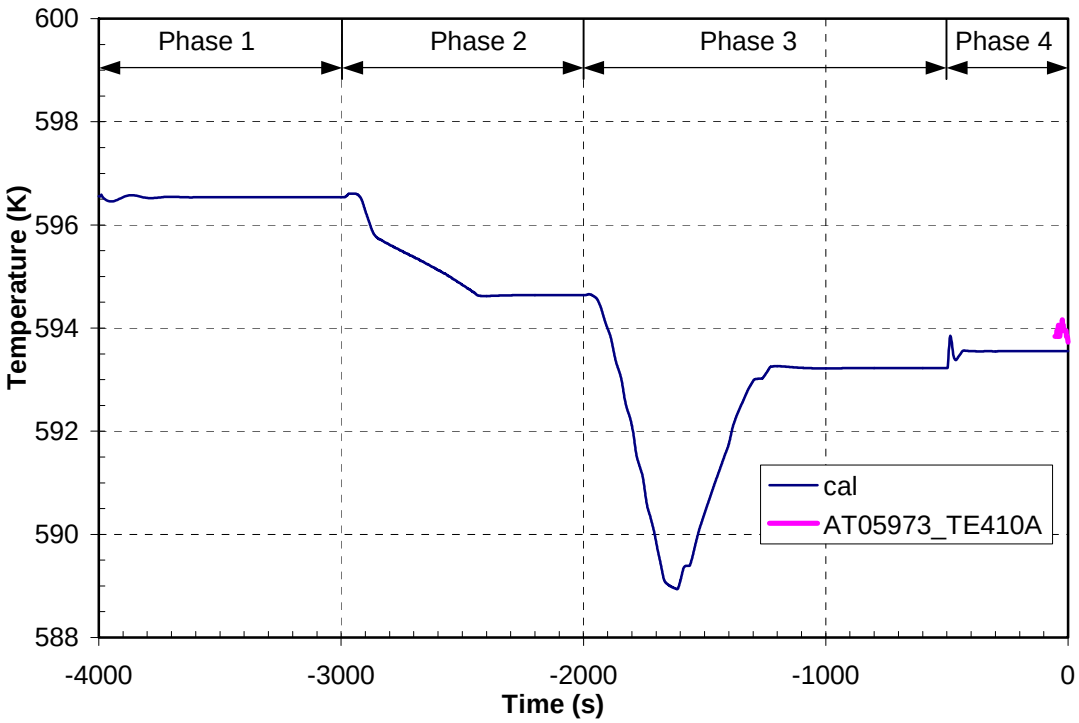


**Figure 8 Hot leg loop 1 temperature—testing of turbine governor valve**

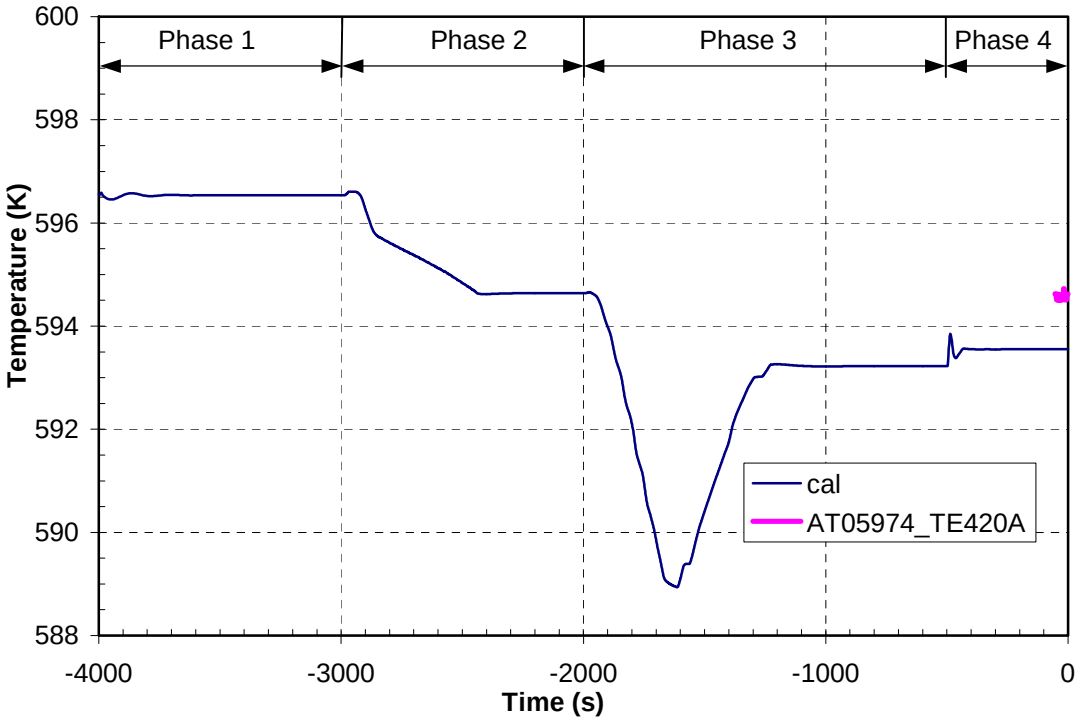


**Figure 9 Hot leg loop 2 temperature—testing of turbine governor valve**

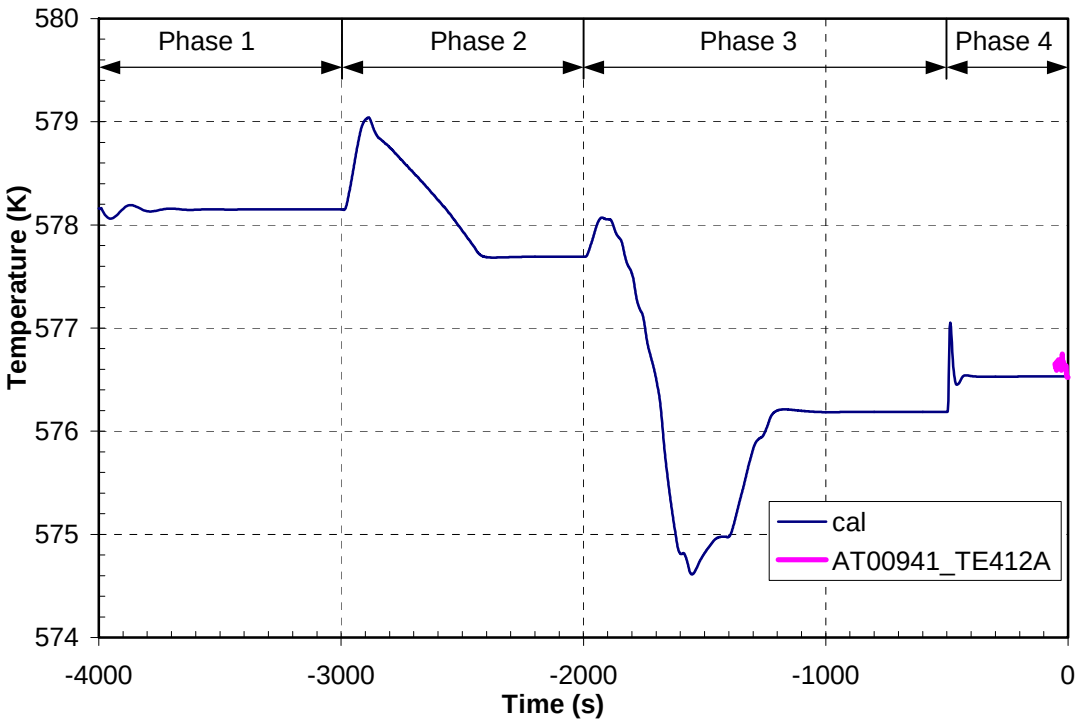


**Figure 10 RCS average temperature—testing of turbine governor valve**

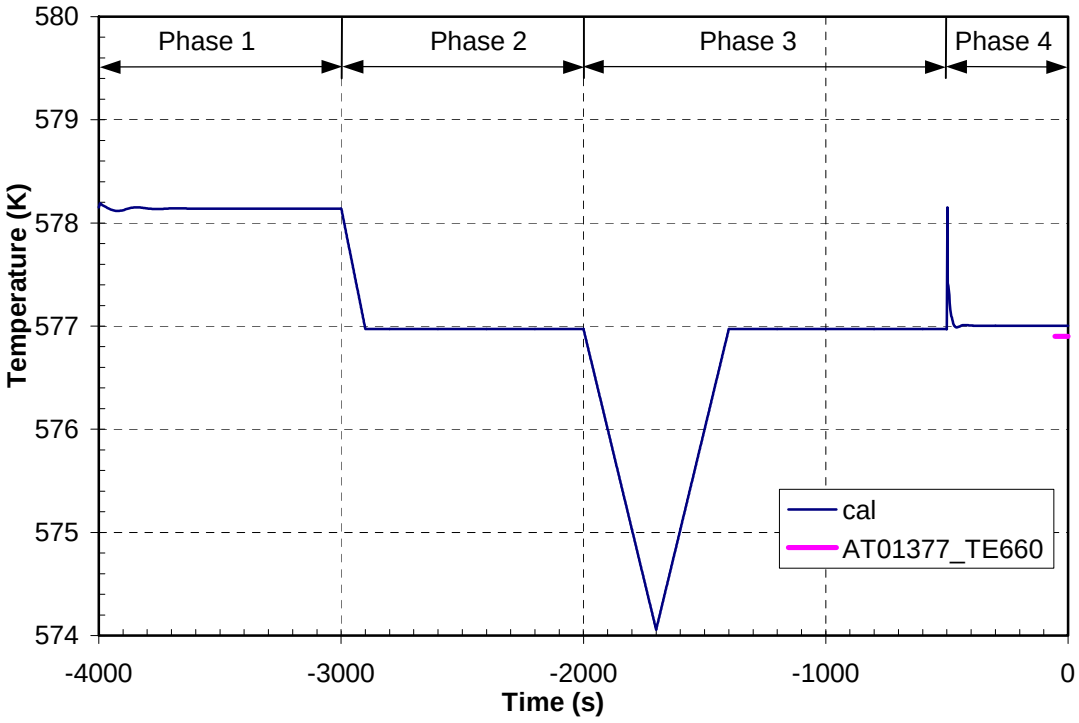


**Figure 11 Reference (programmed) temperature—testing of turbine governor valve**

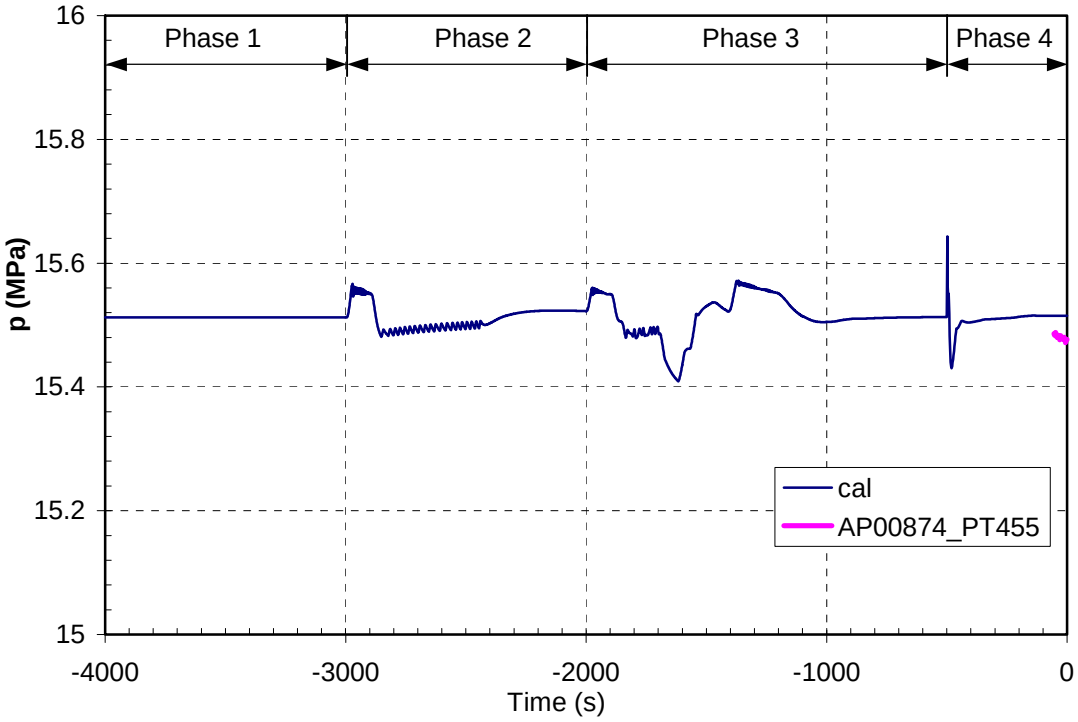


**Figure 12 PRZ pressure—testing of turbine governor valve**

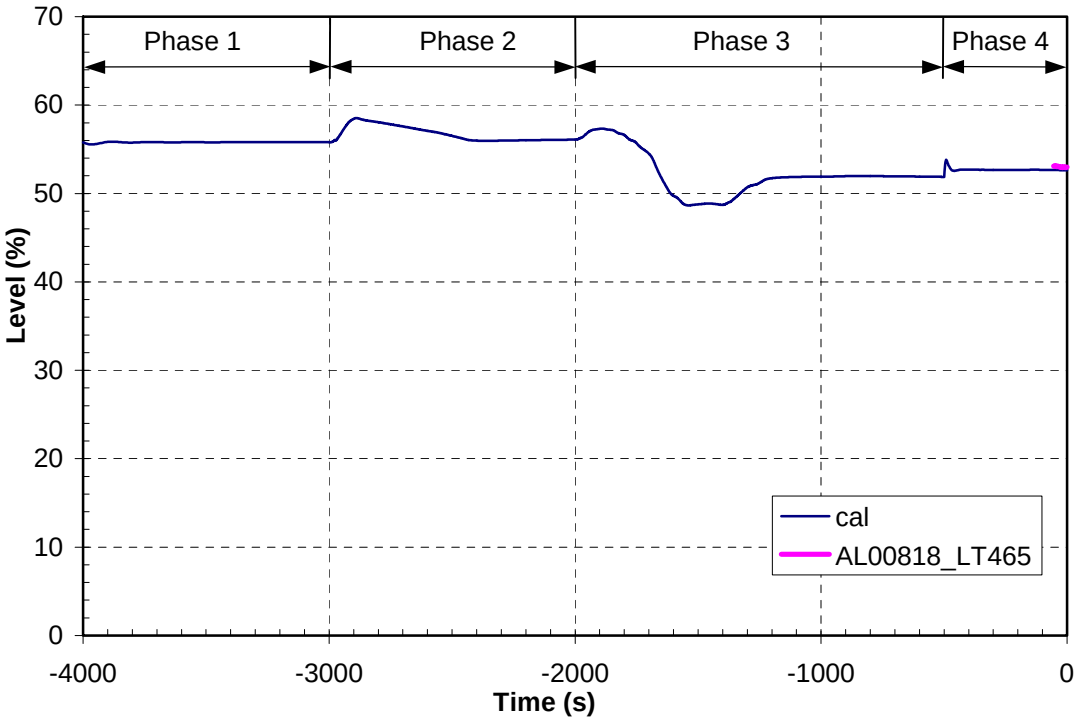


**Figure 13 PRZ level—testing of turbine governor valve**

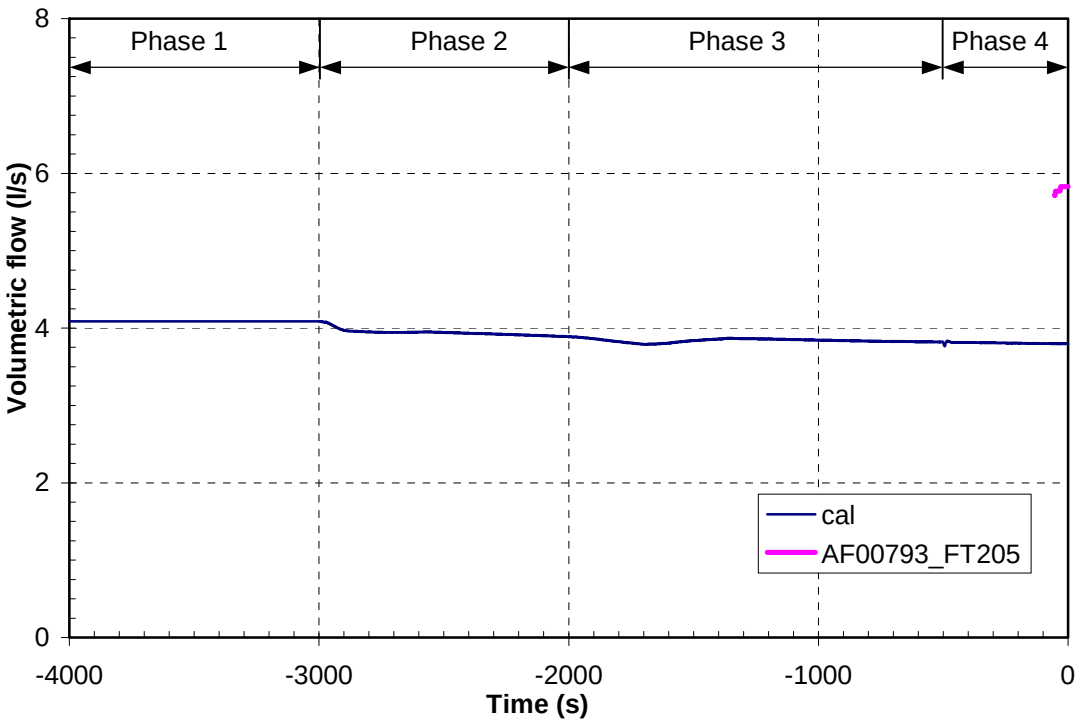


**Figure 14 Charging flow—testing of turbine governor valve**

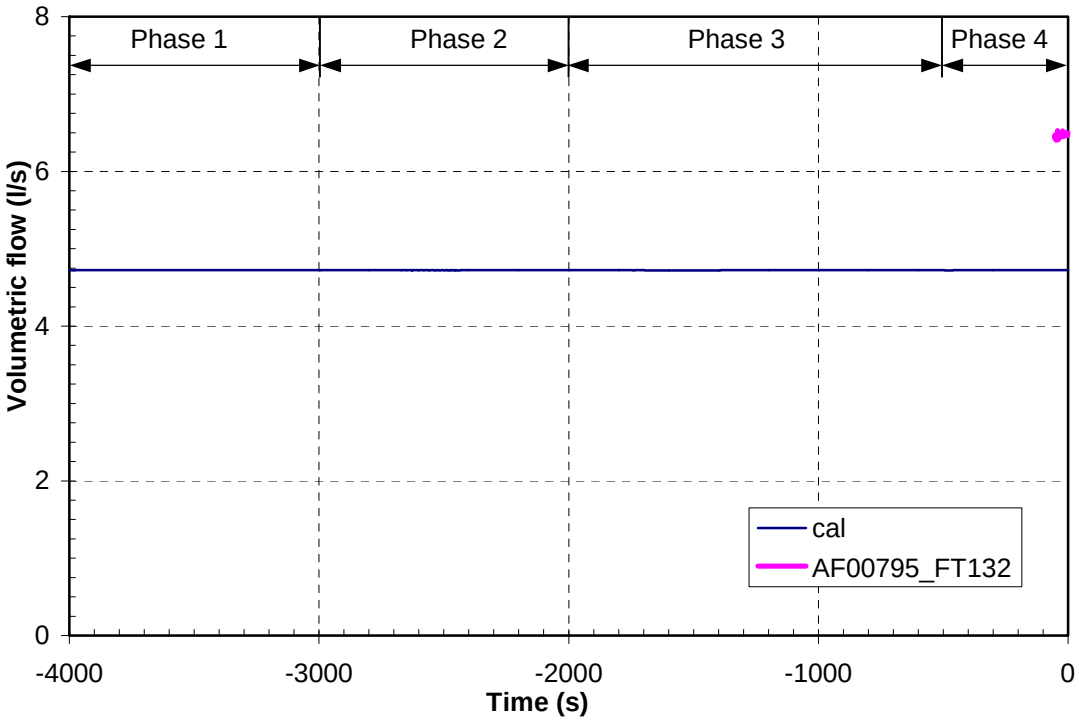


**Figure 15 Letdown flow—testing of turbine governor valve**

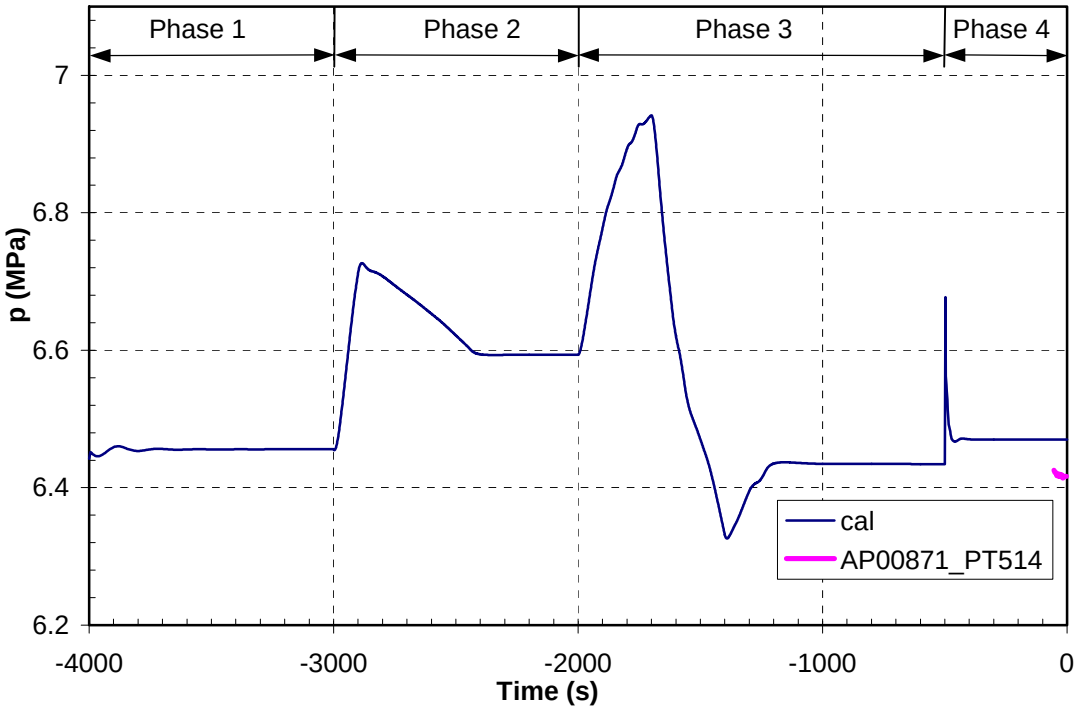


**Figure 16 SG 1 pressure—testing of turbine governor valve**

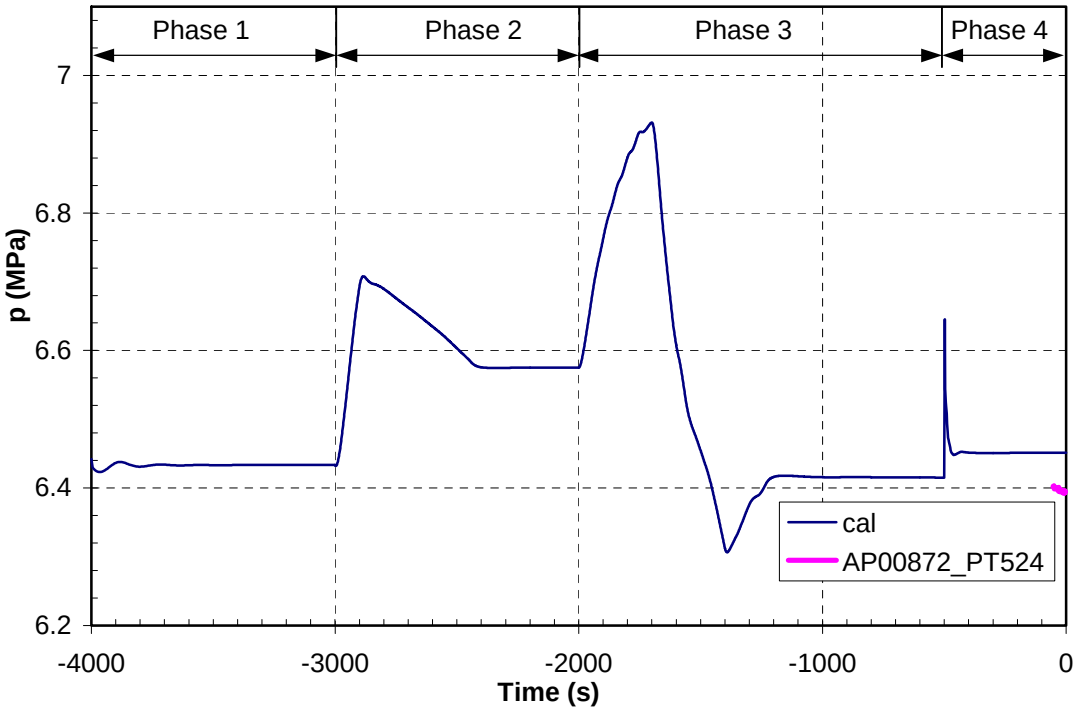


**Figure 17 SG 2 pressure—testing of turbine governor valve**

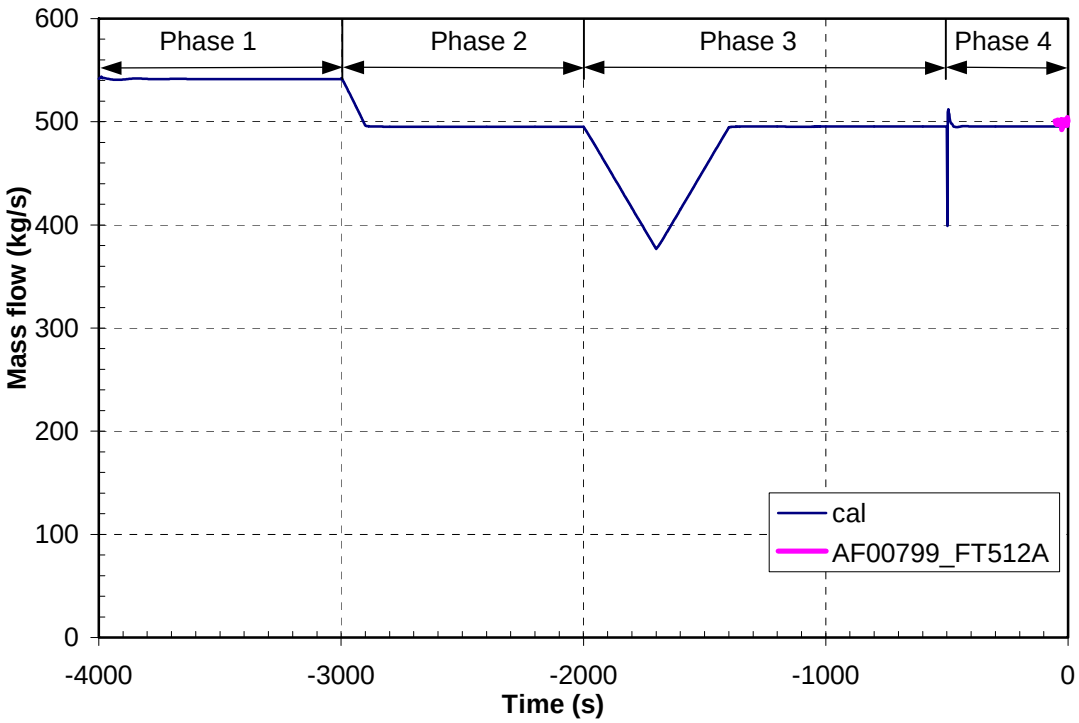


**Figure 18 Steamflow SG 1—testing of turbine governor valve**

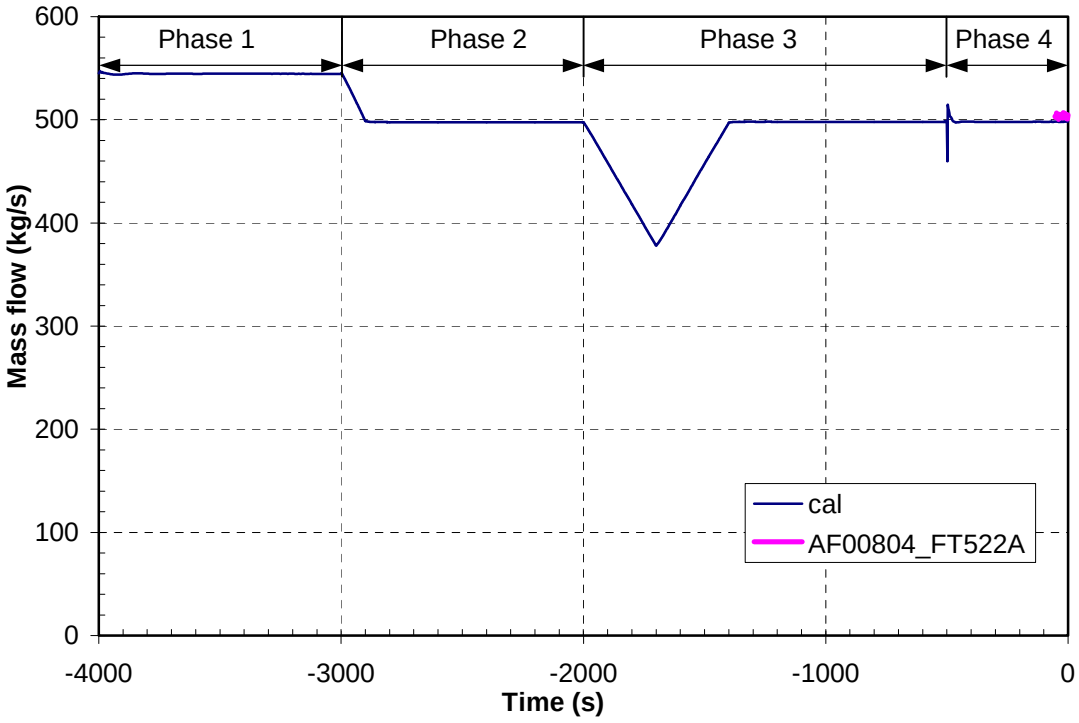


**Figure 19 Steamflow SG 2—testing of turbine governor valve**

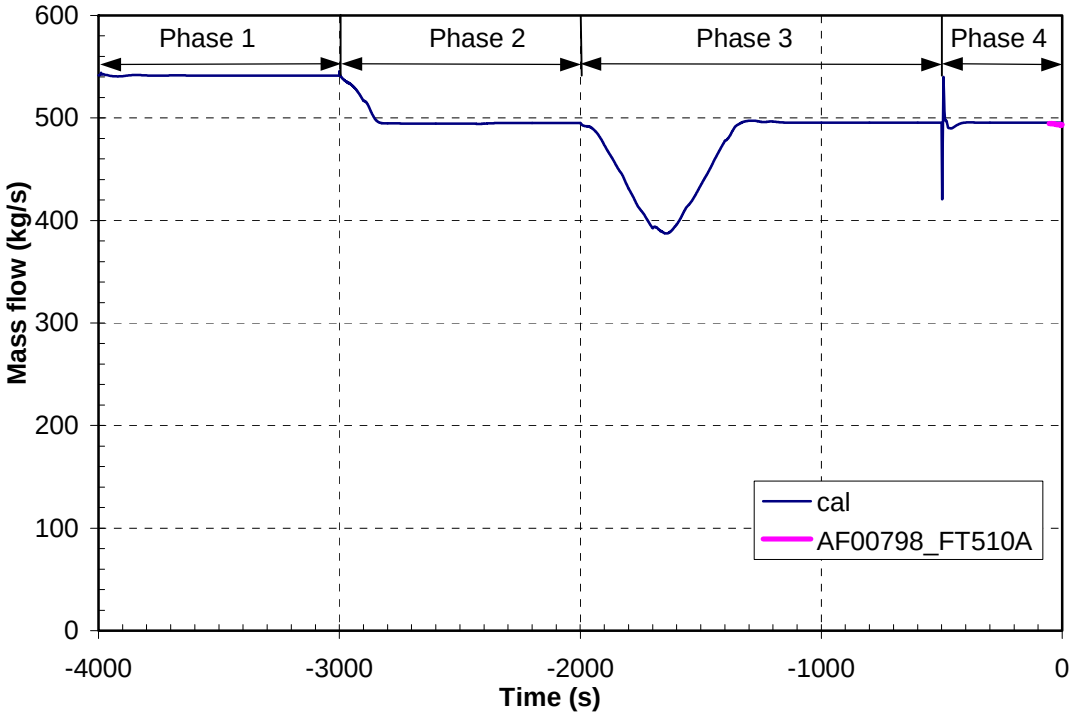


**Figure 20 Feedwater flow SG 1testing of turbine governor valve**

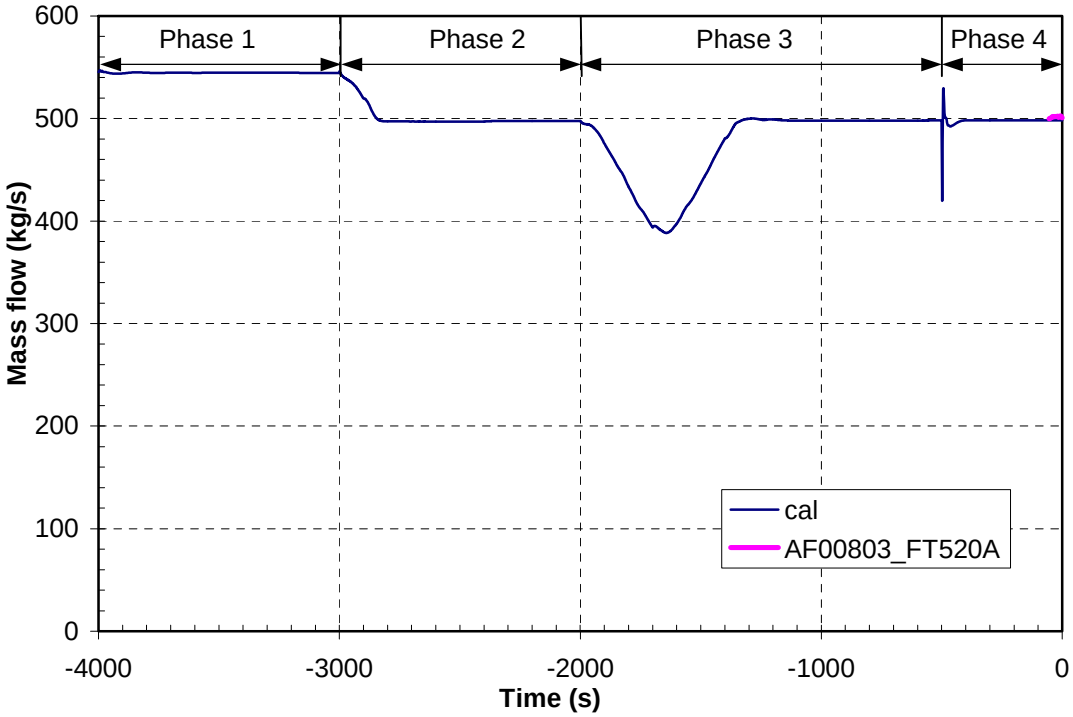


**Figure 21 Feedwater flow SG—testing of turbine governor valve**

## 5.2 Part 2 of the Analysis—Turbine Governor Valve Closure with Reactor Trip

Table 4 presents the time sequence of the main events in the transient. This time sequence was determined based on measured data of plant variables. Measured data showed that the turbine governor valves were closing for 5 seconds—from the 35.5-percent to the 12.2-percent position—and then stabilized for 12 seconds. When the position started to increase to 14 percent, based on operation action, full closure of the turbine valves occurred, causing a turbine trip. The power level showed that the reactor was tripped. The reason for the reactor trip was low steamline pressure, which generated an SI signal. The low steamline pressure resulted from the turbine flow increase (note that data were available for each 2-second increment). At t = 15 seconds, the valve position was 12.2 percent, and at t = 17 seconds, the valve position was already 14.1 percent. Therefore, it was assumed that the operator started to open the turbine governor valves at t = 16 seconds. The SI signal also resulted in the generation of MFW isolation and MSIV signals; the HPIS was actuated, and letdown and charging were isolated. Note that the sequence of events for the plant was determined from measured data, which were used for the plots presented in the figures that follow; therefore, the values are rounded to seconds. For example, the core power starts to drop after 19 seconds. The exact time of reactor trip could not be determined because signal delay and rod drop time is not known exactly.

**Table 4 Time Sequence of Main Events during Transient**

| Event | Measurement | Calculation |
|---|---|---|
| Turbine flow reduction | 0–5 s | 0–5 s |
| Operator action (start of governor valve opening) | 16 s | 16 s |
| SI signal on low steamline pressure | 17 s* | 16.7 s |
| SI pump injection start | 21 s | 20 s |
| SG PORV opening | 27 s | 31 s |
| AFW flow actuation | 42 s | 42 s |

* Based on a 25-second delay of AFW actuation

The transient data available spanned a total of 1,825 seconds. Because the event following turbine valve closure happened very quickly, the plots for the Phase 5 analysis are shown for the following three time windows:

(1) Window 1 (t = −50 seconds to t = 50 seconds): Reactor trip with SG pressure increase and SG PORV opening

(2) Window 2 (t = −50 seconds to t = 450 seconds): SG pressure decrease and primary pressure increase

(3) Window 3 (t = −50 seconds to t = 1,825 seconds): SG pressure increase followed by SG pressure stabilization

Figures 22 thorough 44 present the results of the Phase 5 analysis. For the plant variables identification, refer to Table 3.

Figure 22 represents the core power. The power drops when the reactor is tripped and the rods start to drop. The measurement of the power range channel is based on the neutron flux. After

reactor shutdown, only part of the decay heat is due to neutron flux from delayed neutrons and spontaneous fission neutrons. Decay heat also results from other sources, such as unstable fission products and unstable actinides. Therefore, the measured flow is lower than the actual flow, which is the major reason for the disagreement between the measured data and the calculation. In Figure 22(c), it can be seen from the calculated data that the decay heat is simulated with RELAP5, while the measured data do not correctly depict this decay. Figure 23 shows the cold-leg temperature in loop 1, and Figure 24 shows the cold-leg temperature in loop 2. Because of the power mismatch between the reactor and turbine power, the cold-leg temperatures initially increased and then decreased, while the hot-leg temperatures in both loops (Figure 25 and Figure 26) remained practically constant. However, when the reactor was tripped, the hot-leg temperatures began to drop, and the cold-leg temperatures started to increase. These temperature values approach each other because the difference between the hot- and cold-leg temperatures is smaller after reactor trip (i.e., just a few degrees K).

Figure 27 shows the RCS average temperature. After transient initiation, the temperature starts to increase until the reactor is tripped at t = 17 seconds. At this point, the temperature is a function of the primary system cooling (by primary-side injection) and the secondary-side heat sink. The secondary-side heat sink dominates; therefore, the shape of the RCS average temperature plot is similar to the plots of both SG pressure trends (see Figure 33 and Figure 34). The reference temperature shown in Figure 28 corresponds to turbine power. As in the RELAP5 input model, the turbine is not explicitly modeled; the reference temperature follows the turbine flow. When the turbine flow was reduced, the reference temperature decreased initially. When the operator opened the turbine valves, the turbine flow increased until the reactor tripped. Then, the flow dropped to no load conditions. The measured reference temperature follows the turbine load (impulse pressure). The comparison is relevant only to the time of reactor trip. Also, in the presence of steam dump flow, the turbine flow could not be determined accurately based on total steamflow. The calculated reference temperature could be simulated correctly only in the case in which either the steam dump flow or the turbine flow is known in addition to the steamflow.

Figure 29 shows the PRZ pressure. The model calculates the initial pressure increase very well. The pressure rapidly increases until the PRZ sprays are actuated. It can be seen that continuous sprays efficiently reduced the pressure increase before reactor trip. When the reactor tripped, the PRZ pressure decreased further. Initial agreement between the calculated data and the measured data is very good, including the peak pressure values. However, it can be seen that, after 25 seconds, the calculated pressure indicates a repressurization of the primary system. This may result from earlier SI termination (see Figure 41 and Figure 42). Later agreement between the calculated and measured data is good. The pressure returned to its normal value via the PRZ control system. The sprays were actuated when the pressure began to increase above the spray setpoint, at around t = 650 seconds. At around t = 900 seconds, the operators decided to reestablish charging and letdown flow (see Figure 31 and Figure 32). At around t = 1,500 seconds, the sprays were terminated. Figure 30 illustrates the PRZ level. There was some discrepancy between the calculated and the measured SI flow; however, it was decided not to tune the calculated SI flow to the measured data.

Figure 31 and Figure 32 depict the charging and letdown flow, respectively. Both charging and letdown flow were isolated upon the SI signal in the calculation, although the measured data showed some delay in isolation. After t = 900 seconds, the measured data show that the operators reestablished both charging and letdown (operator action); therefore, the calculations also assumed these flows (note that approximate values were used).

The calculated SG pressures were in good agreement with the measurement data (Figure 33 and Figure 34). The reason for this agreement is partly the AFW flow value, which was based on actual plant measurement (see Figure 43 and Figure 44). The operators were changing the AFW flow as the transient began. However, in the initial period when the AFW was not injecting, the first SG pressure peak resulted from closure of the governor valve, and the second peak resulted from the turbine trip. When the operator opened the turbine governor valves, the SG pressure after the first peak started to decrease, causing an SI signal to be generated based on low steamline pressure. The second peak caused the SG PORV valve to open. To obtain an exact match of SG pressures, the smaller steamflow than measured was modeled as indicated by measured data (Figure 37 and Figure 38).

Following the main steamline isolation after the turbine trip, there was some steamflow to the gland steam system. Because the steam is generated based on available heat (mostly decay heat), the model indicated the maximum value of generated steam, which was lower than the measured data (labeled “cal. limiting”). Therefore, the steamflow was tuned to obtain as good a match to the measured SG pressure as possible. The value of steamflow is physically reasonable, but it is not known if this value reflects the reality of the transient. In addition, the transient was very sensitive to this variable. Without assuming the measured steamflow after reactor trip or the measured data for steamflow, the SG pressure would be overpredicted (requiring SG PORV opening) or underpredicted. Only these variables required tuning; all other calculated variables were in excellent agreement with measured variables. The analysis revealed an important finding—the RELAP5 computer code calculation suggested some steamflow to the gland steam system. It was later discovered that there is greater steamflow to the gland steam system when steamline isolation occurs following a turbine trip. This particular circumstance occurred in the analyzed event. The base input model did not include the steamflow to the gland steam system.

The SG levels also agreed well initially (see Figure 35 and Figure 36). The reactor trip caused both turbine trip and MFW isolation. The closure of the turbine valves and core heat transferred to the SG resulted in the steam pressure increase (see Figure 33 and Figure 34), which had a shrink effect on the SG-level instrumentation (see Figure 35 and Figure 36). Upon an SI signal, following a 25-second delay, the AFW injection was started to remove the decay heat and fill the SGs. Following the MFW isolation, the SG level was affected by AFW and released steam. However, it was observed that, in the time period between t = 26 seconds and t = 73 seconds and t = 70 seconds, when SG PORVs 1 and 2 were operated, respectively, the calculated level is higher than the measured data. In addition, level oscillates were observed around the measured trend until t = 1,000 seconds due to oscillating steamflow. One possible explanation for this behavior could be that the RELAP5 input model underpredicted the damping of the oscillating water flow between the downcomer and the riser in the SG.

Figures 37 through 40 illustrate the steamline and feedwater flows. Most important is the initial phase. It can be seen that, in the calculation, the SI signal was generated immediately after the turbine valve closure, while the measured data showed some delay. Nevertheless, the major phenomena were simulated, and the steamflow values matched very well. Although the steam dump opened, no measured data were available for steam dump flow. The steamflows in both steamlines (Figure 37 and Figure 38) represent the flow to both the steam dump and turbine. As mentioned earlier, the measured values of steamflows are not reliable after reactor trip upon an SI signal.

Similarly, the feedwater flow is not correct in the time interval immediately after reactor trip. The feedwater isolation valves closed upon the SI signal. The measured feedwater flow data shown Figure 39 and Figure 40 indicate some flow after reactor trip. As shown in Figure 41 and Figure 42. the calculated SI flow was lower than the plant-measured data. The spike in calculated data resulted from the initial surge of injection flow into the reactor vessel. As discussed previously, the disagreement between the calculated and measured data has some influence on the PRZ level shown in Figure 30.

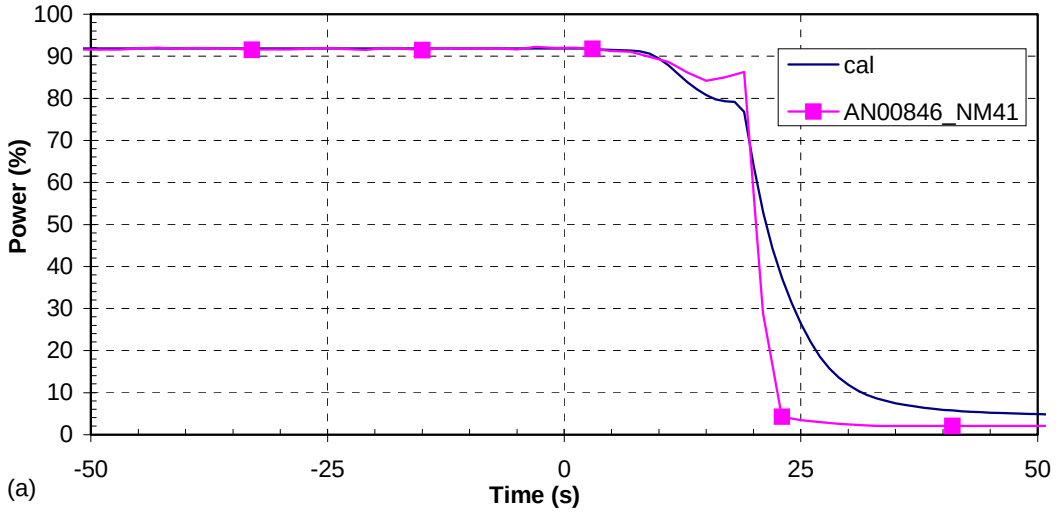


(a)

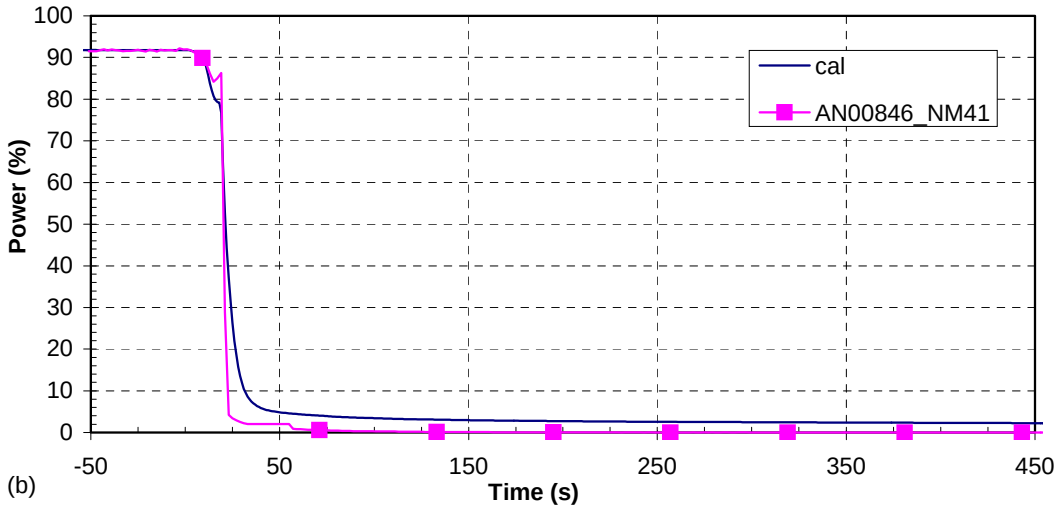


(b)

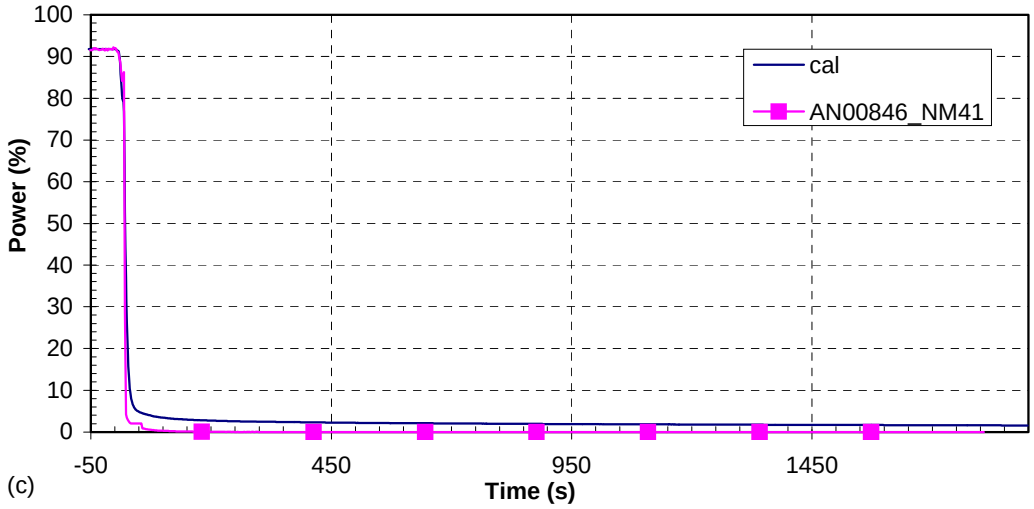


(c)

**Figure 22 Core power—turbine governor valve closure with reactor trip**

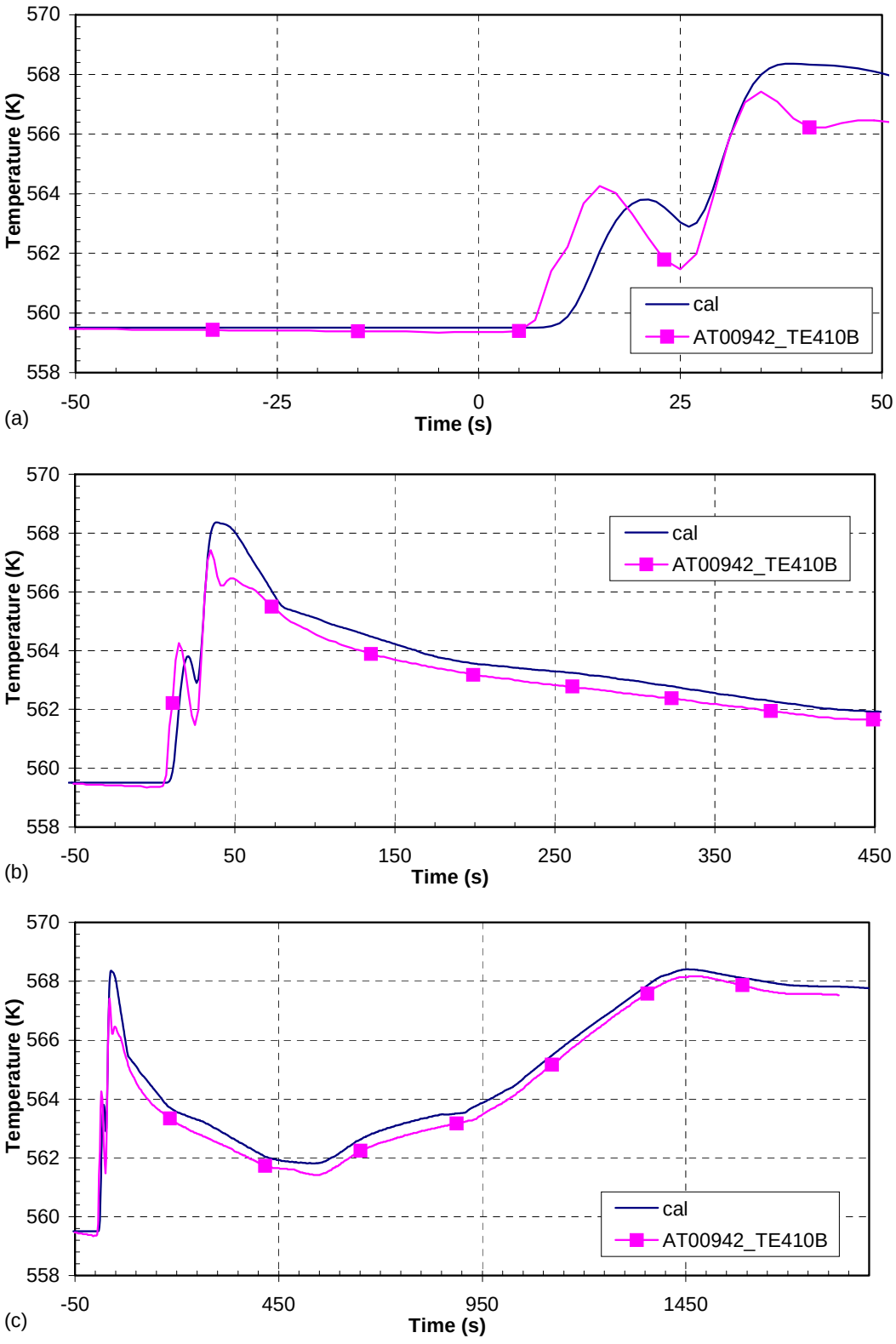


**Figure 23 Cold leg loop 1 temperature—turbine governor valve closure with reactor trip**

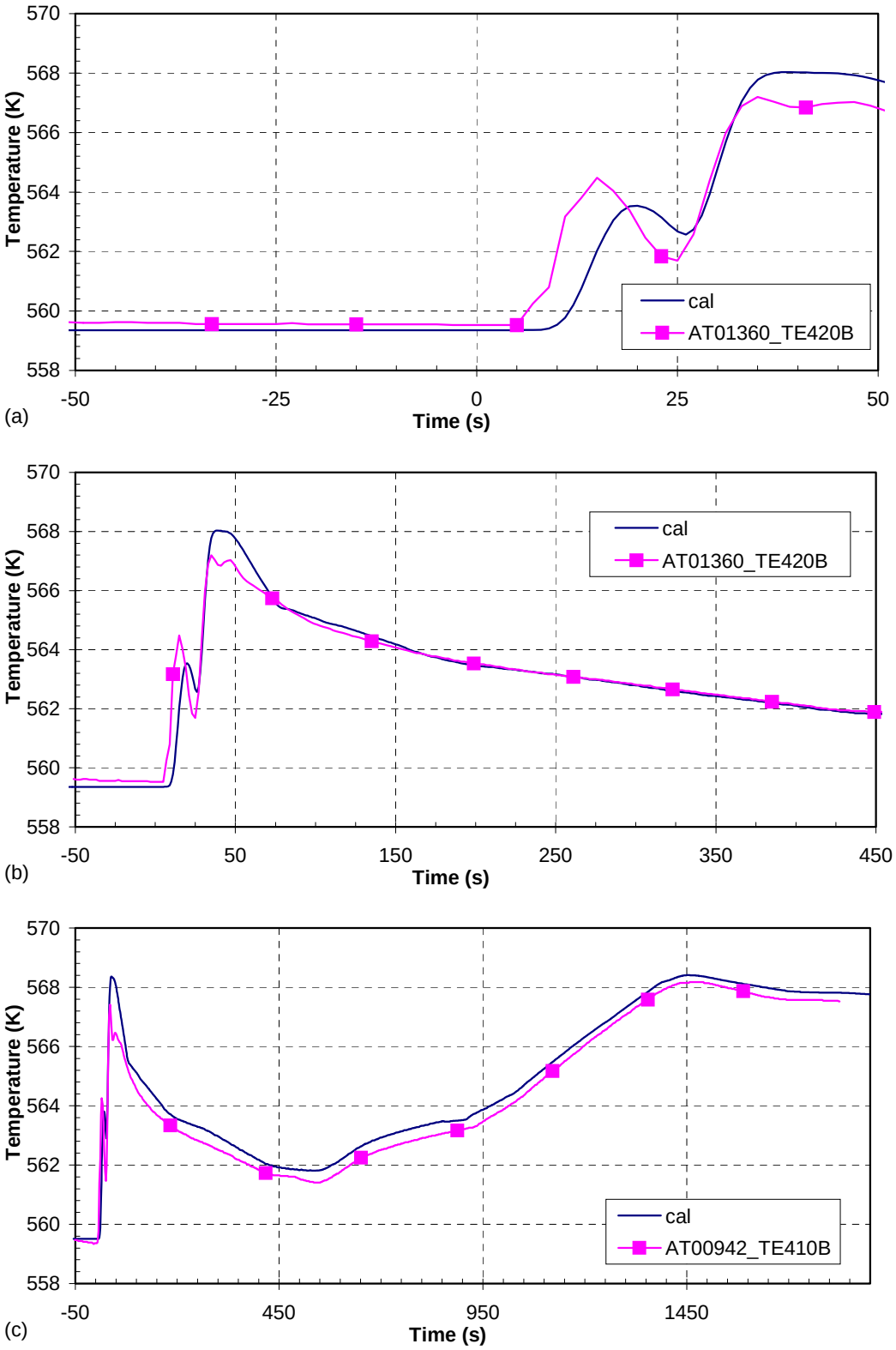


**Figure 24 Cold leg loop 2 temperature—turbine governor valve closure with reactor trip**

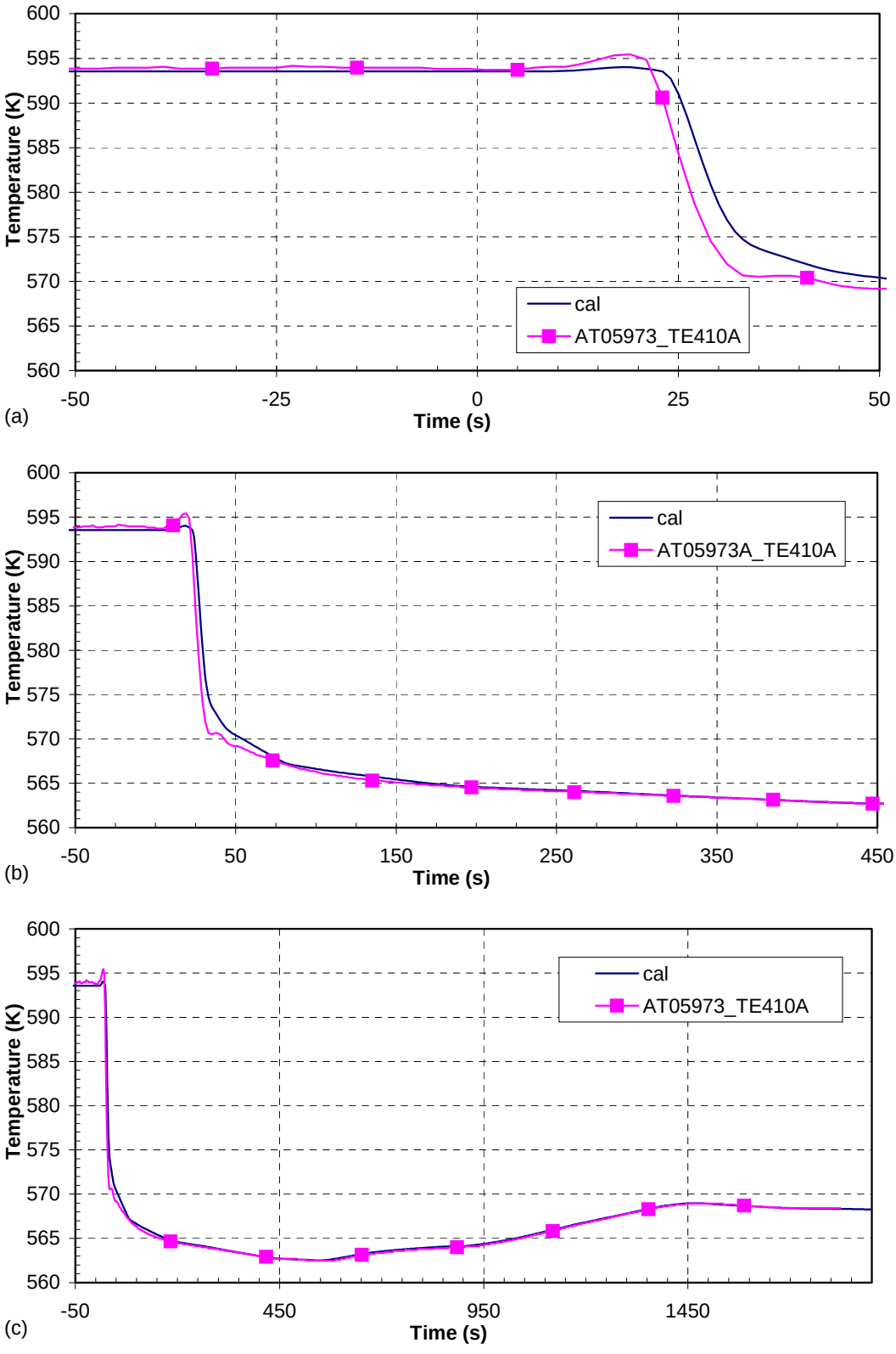


**Figure 25 Hot leg loop 1 temperature—turbine governor valve closure with reactor trip**

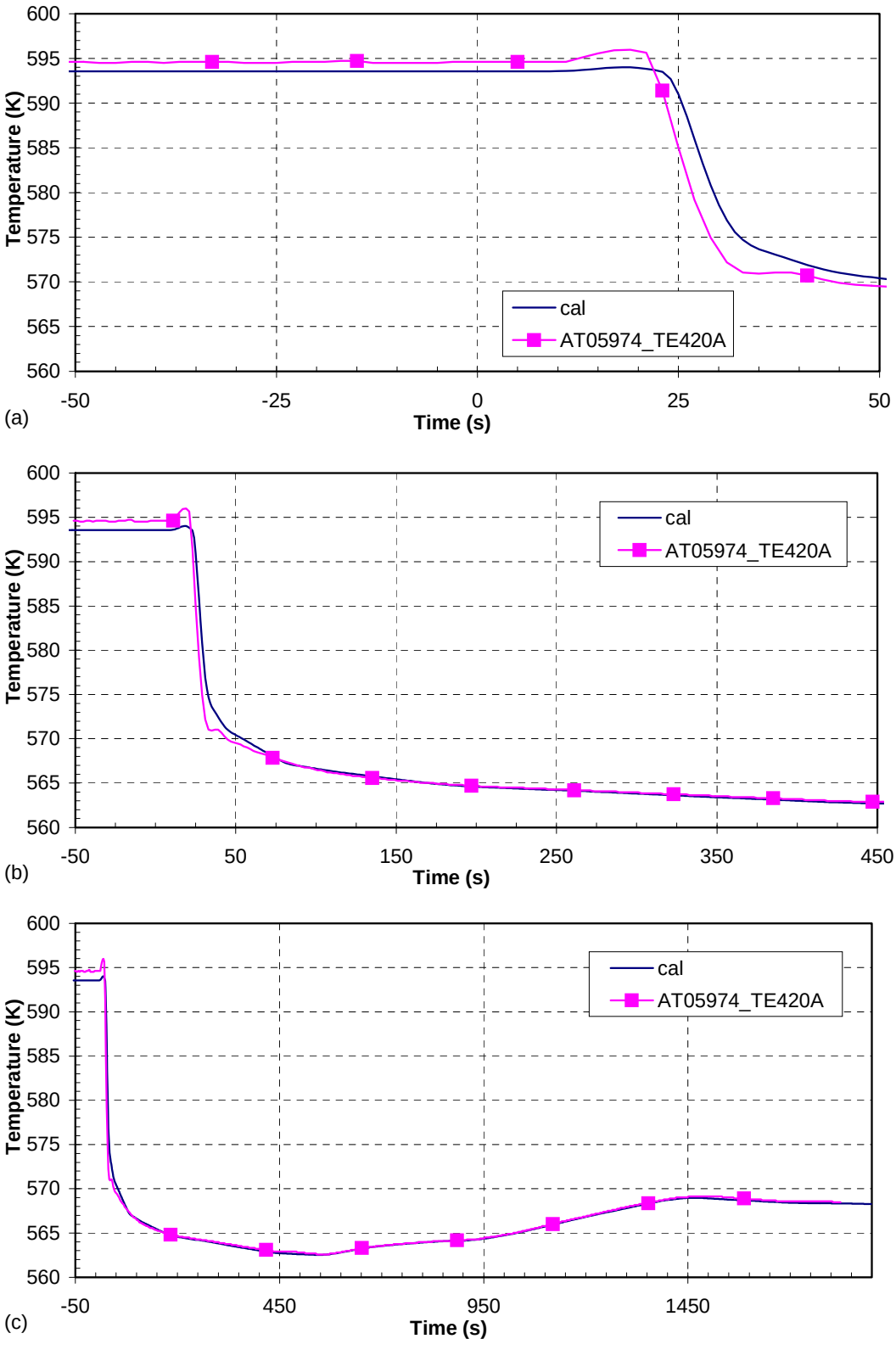


**Figure 26 Hot leg loop 2 temperature—turbine governor valve closure with reactor trip**

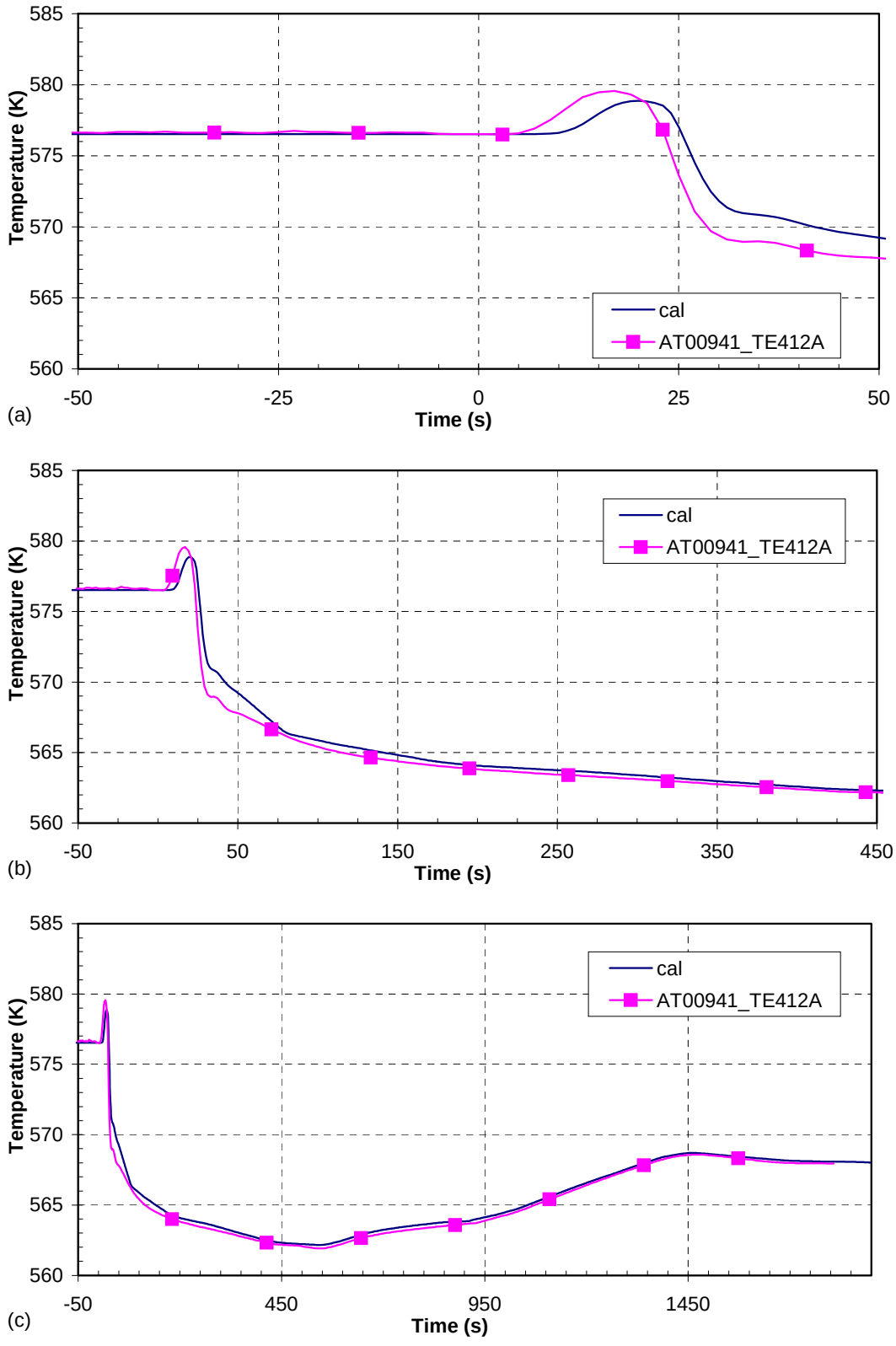


**Figure 27 RCS average temperature—turbine governor valve closure with reactor trip**

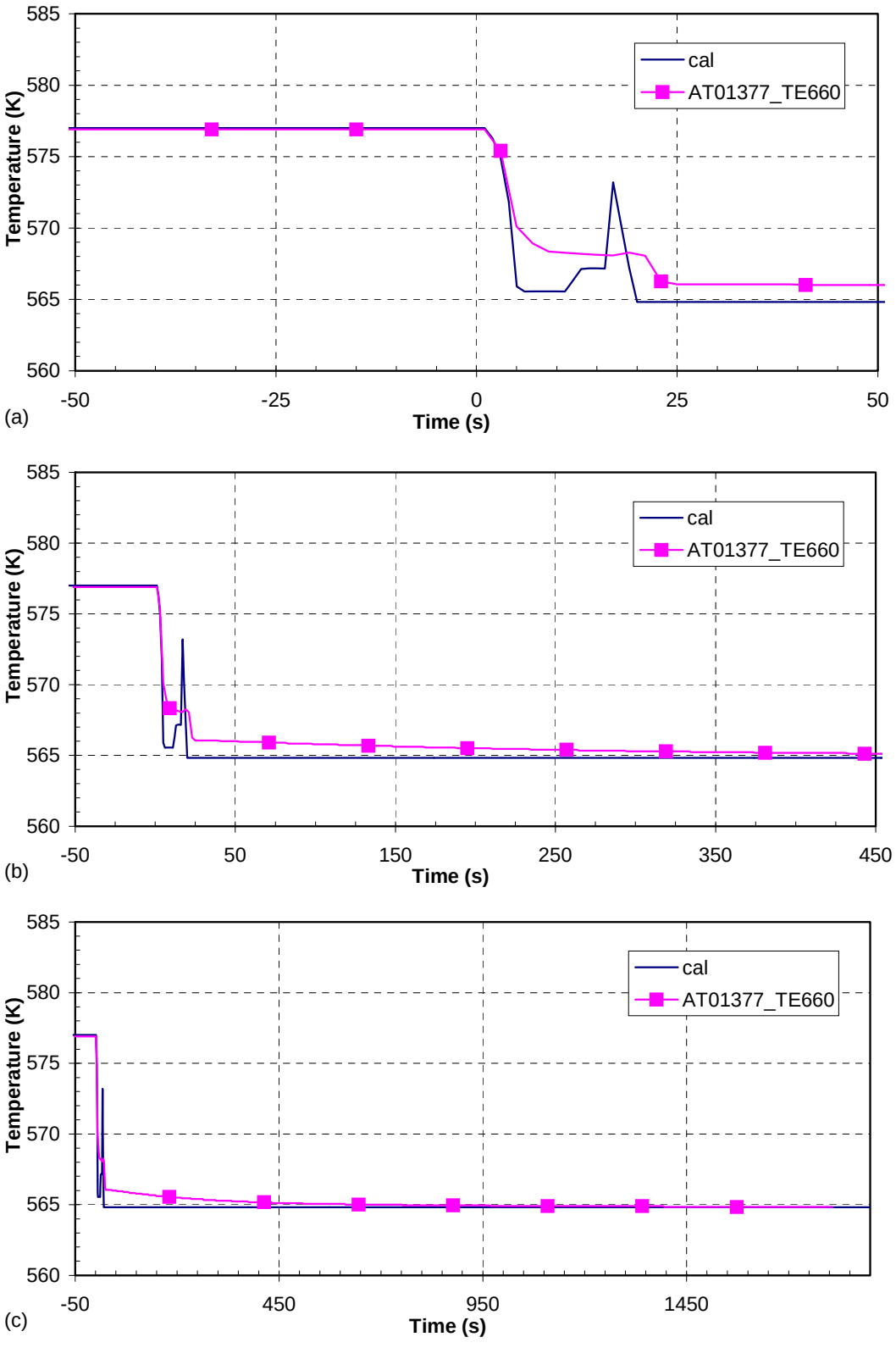


**Figure 28 Reference temperature—turbine governor valve closure with reactor trip**

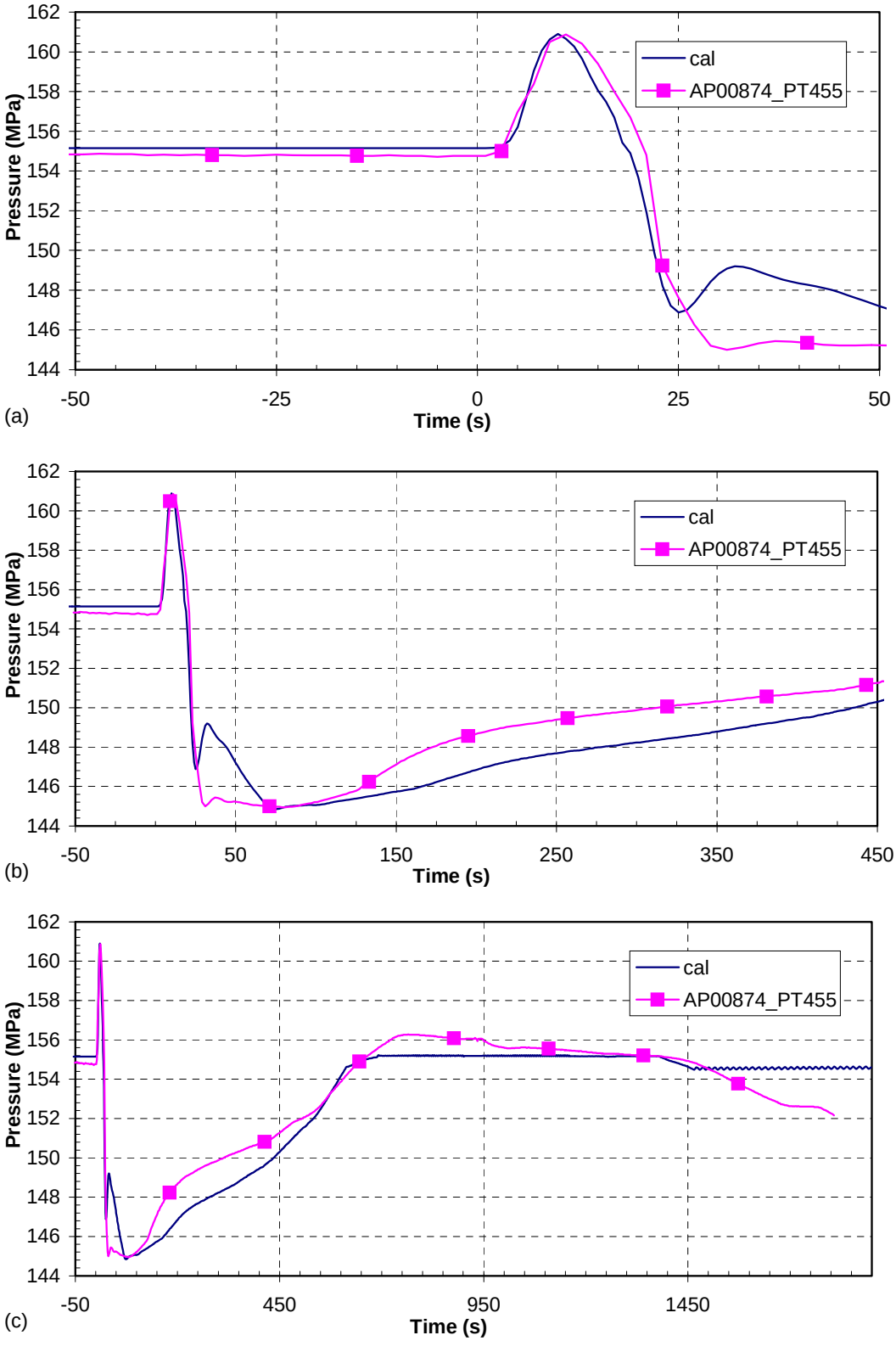


**Figure 29 PRZ pressure—turbine governor valve closure with reactor trip**

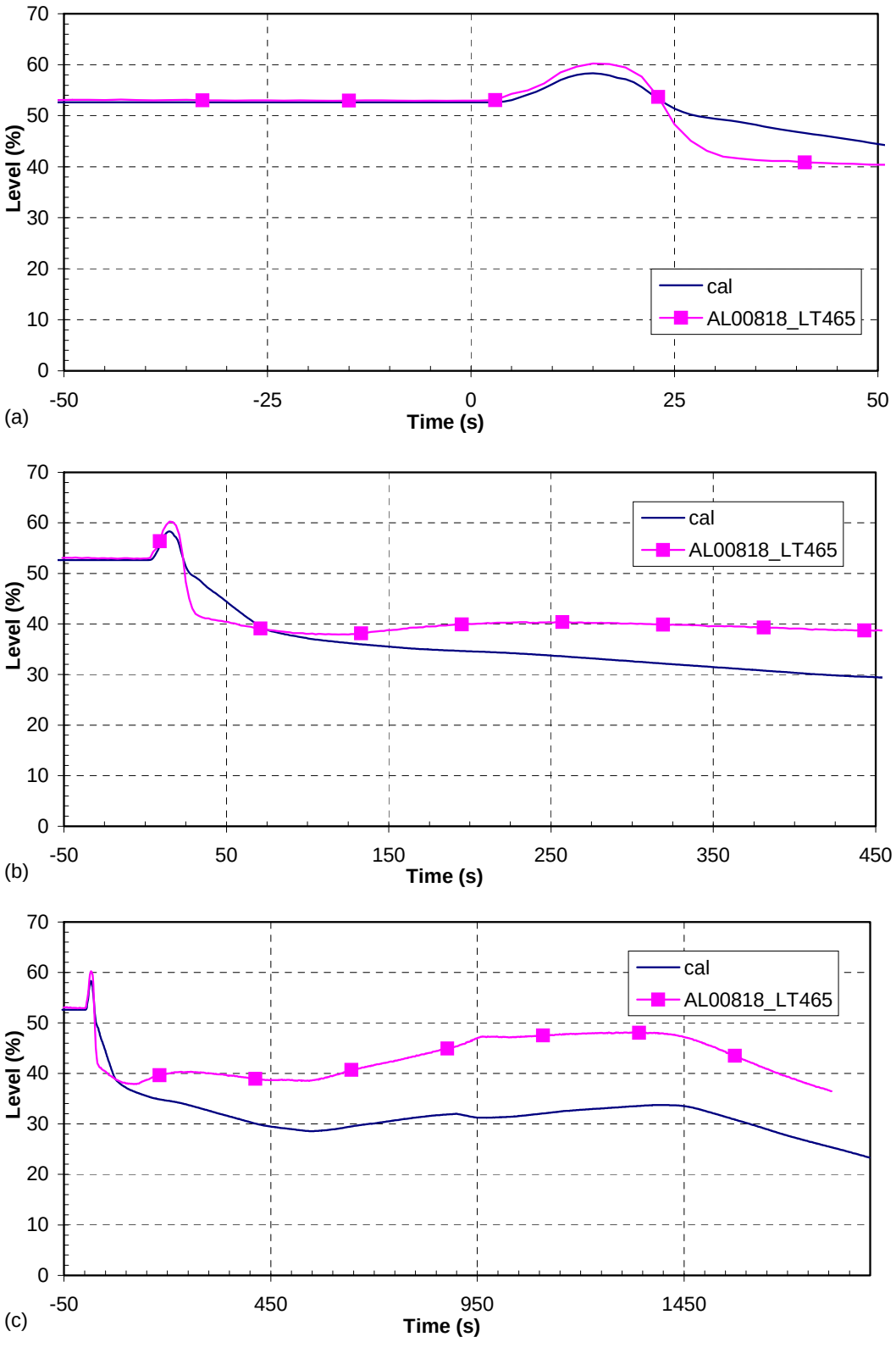


**Figure 30 PRZ level—turbine governor valve closure with reactor trip**

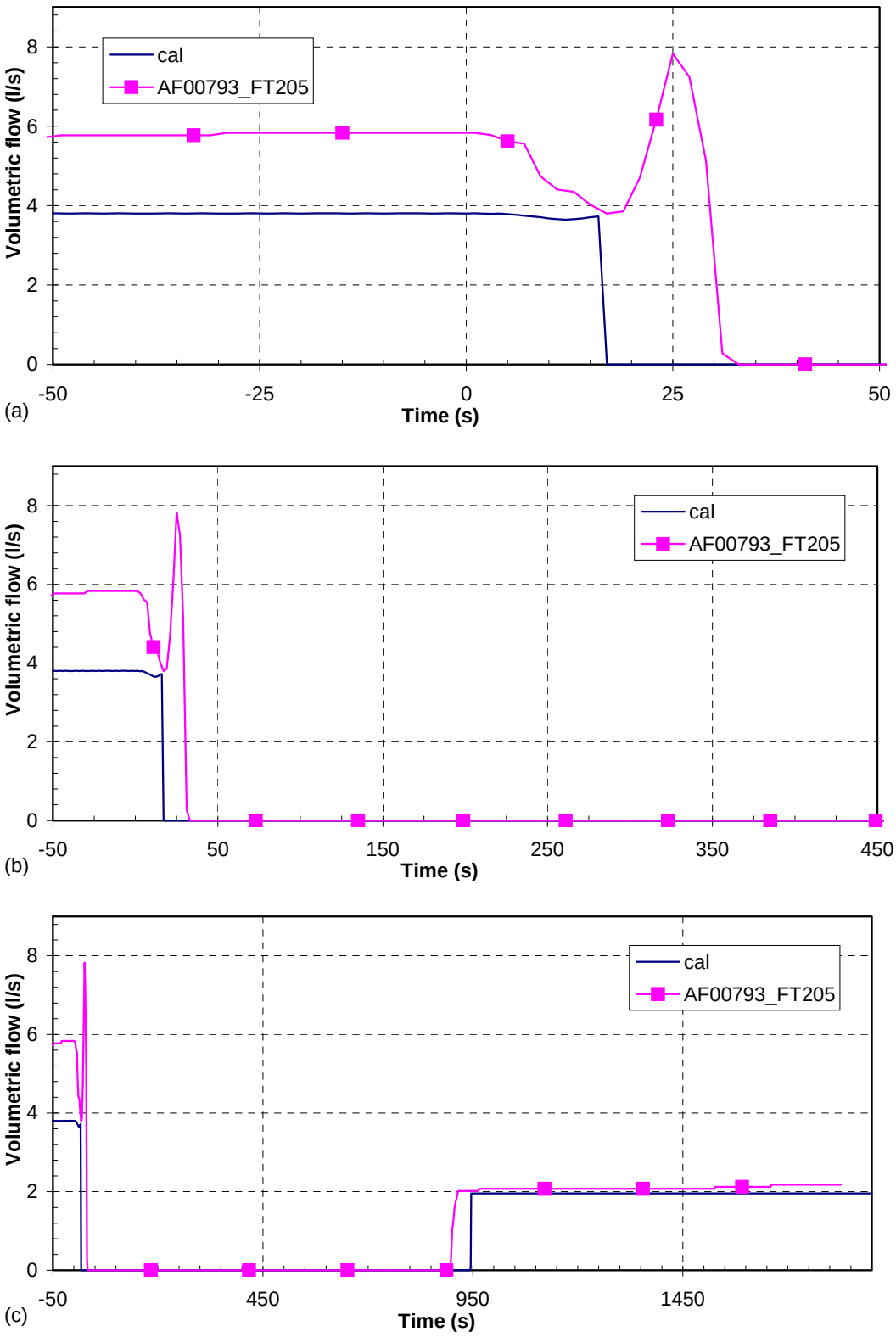


**Figure 31 Charging flow—turbine governor valve closure with reactor trip**

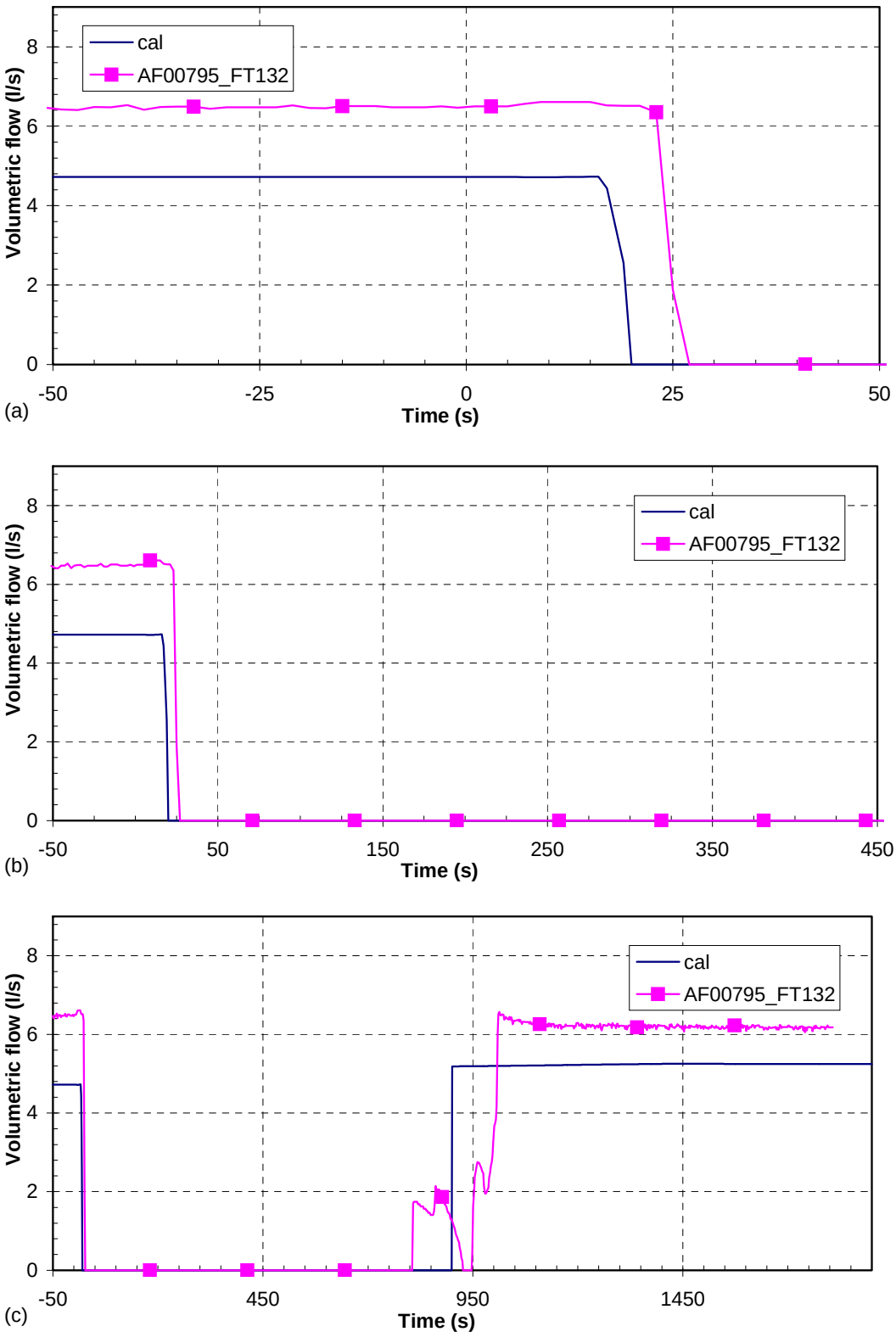


**Figure 32 Letdown flow—turbine governor valve closure with reactor trip**

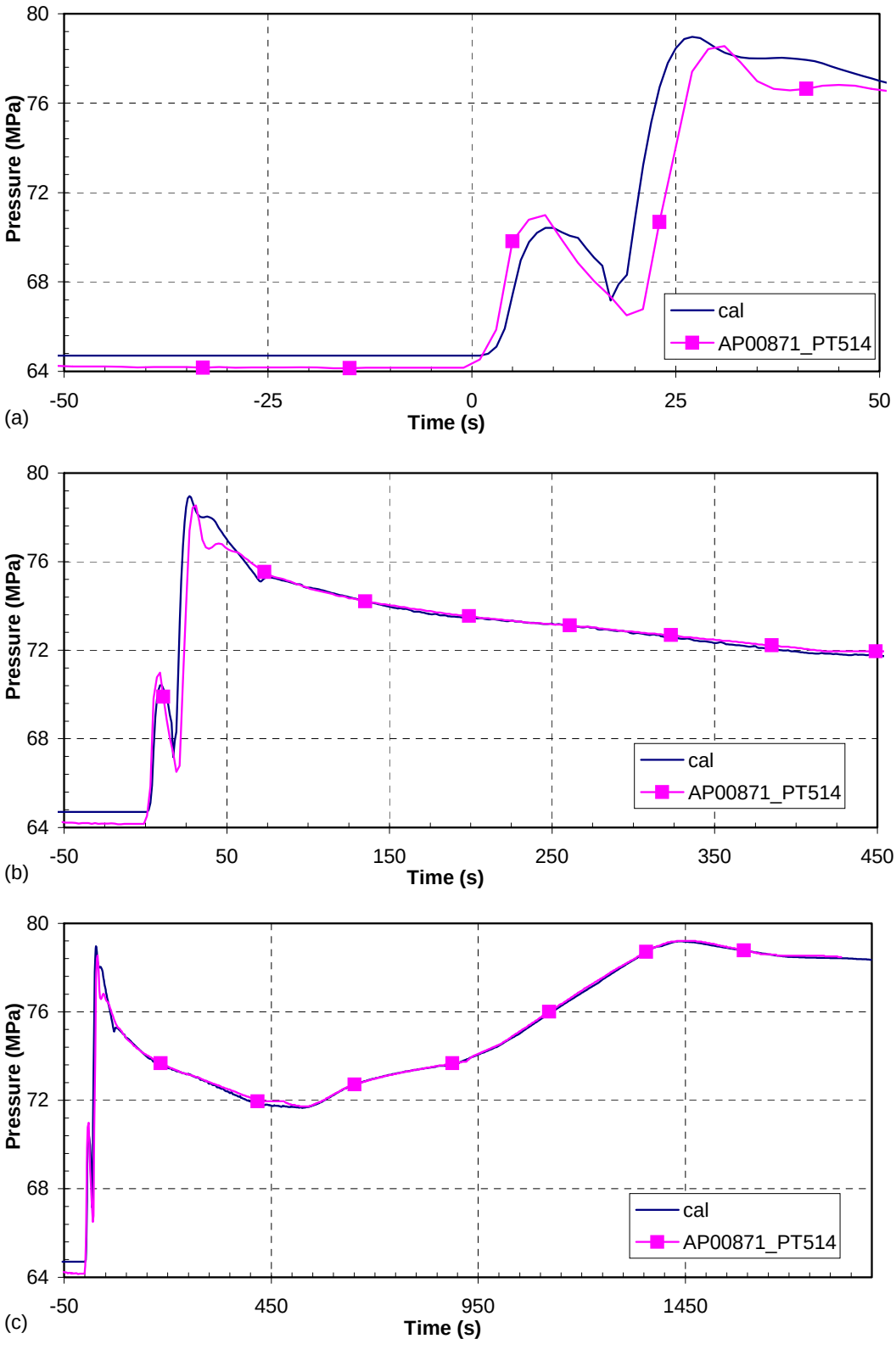


**Figure 33 SG 1 pressure—turbine governor valve closure with reactor trip**

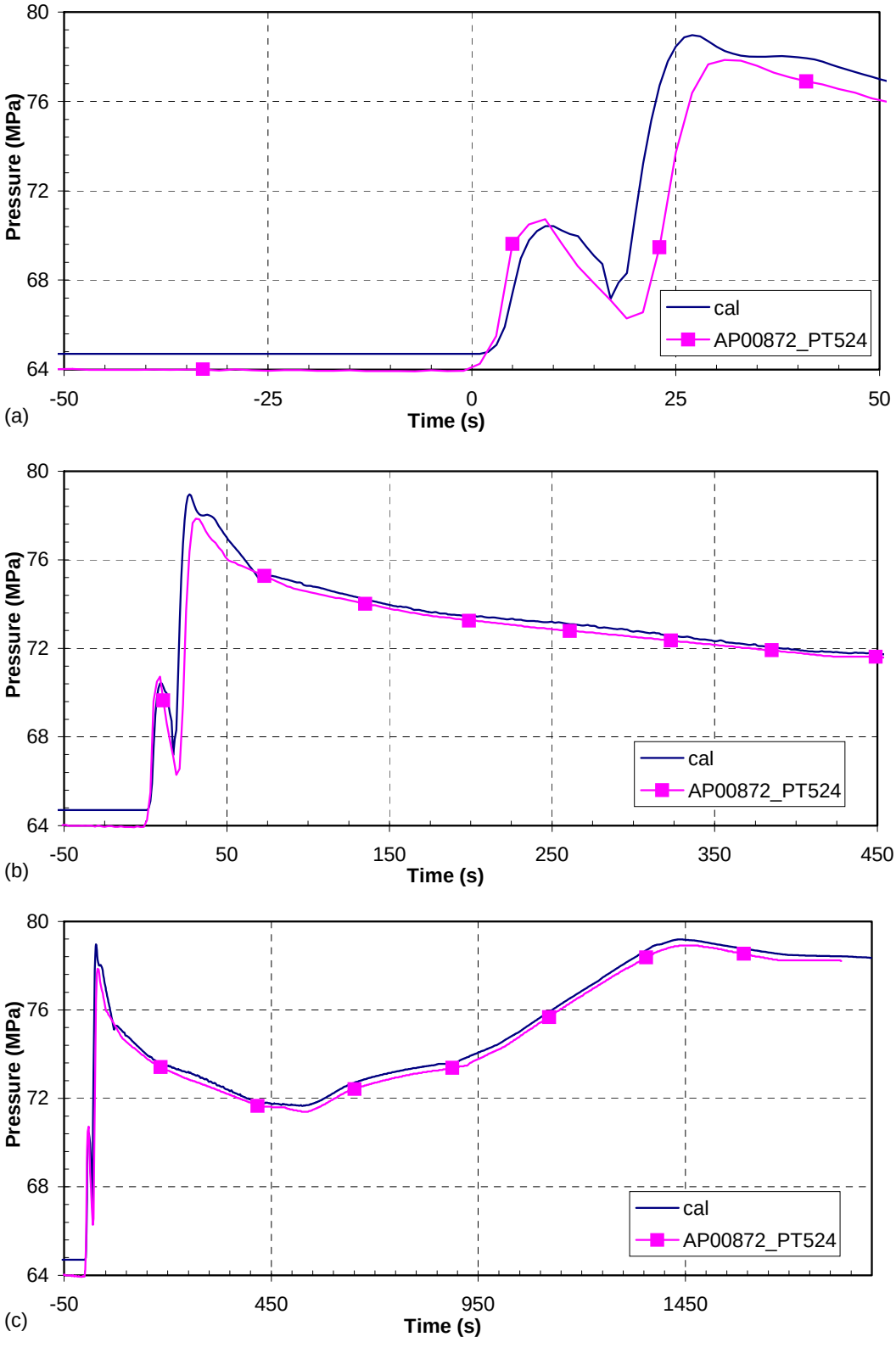


**Figure 34 SG 2 pressure—turbine governor valve closure with reactor trip**

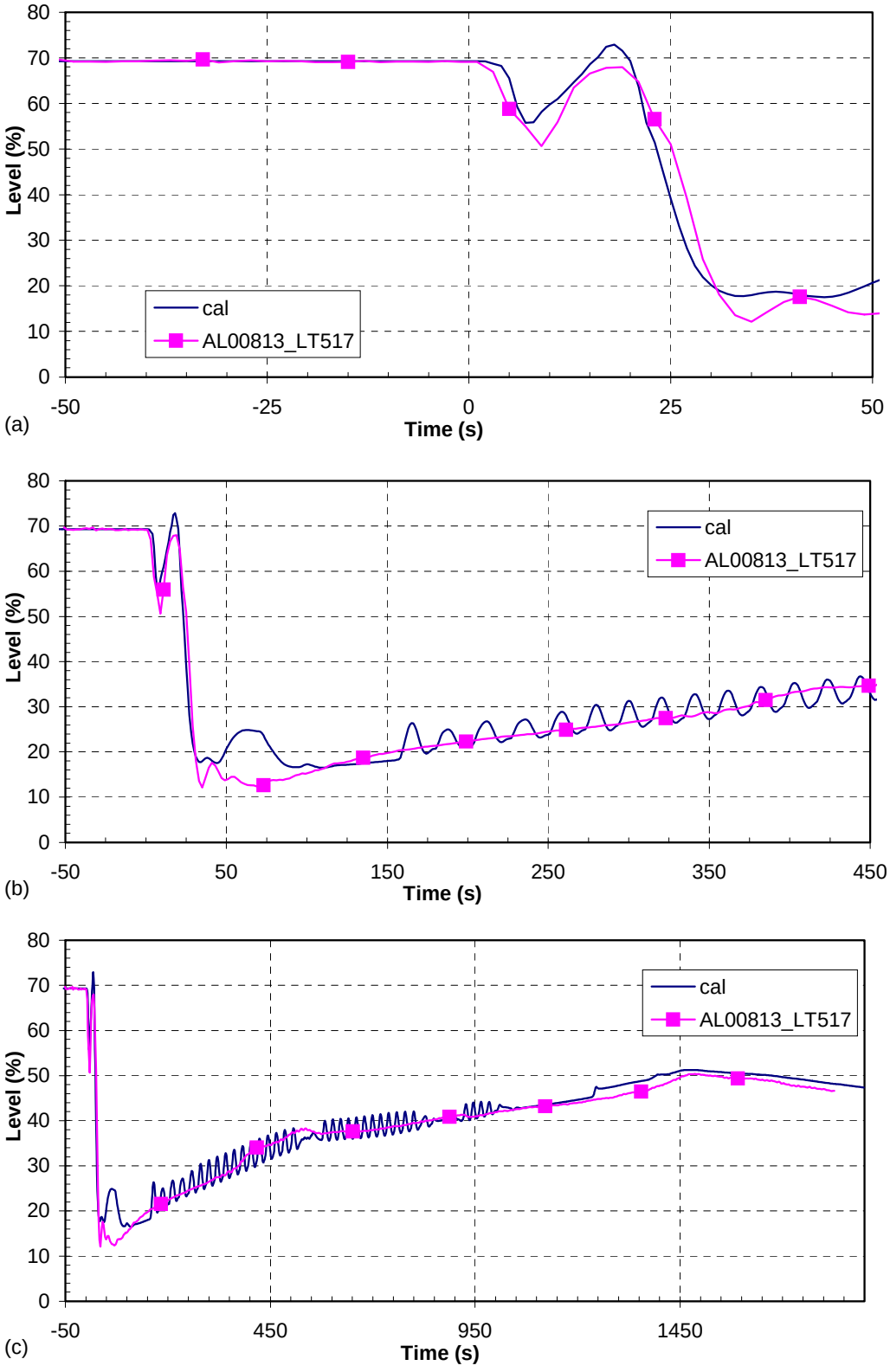


**Figure 35 SG 1 narrow range level—turbine governor valve closure with reactor trip**

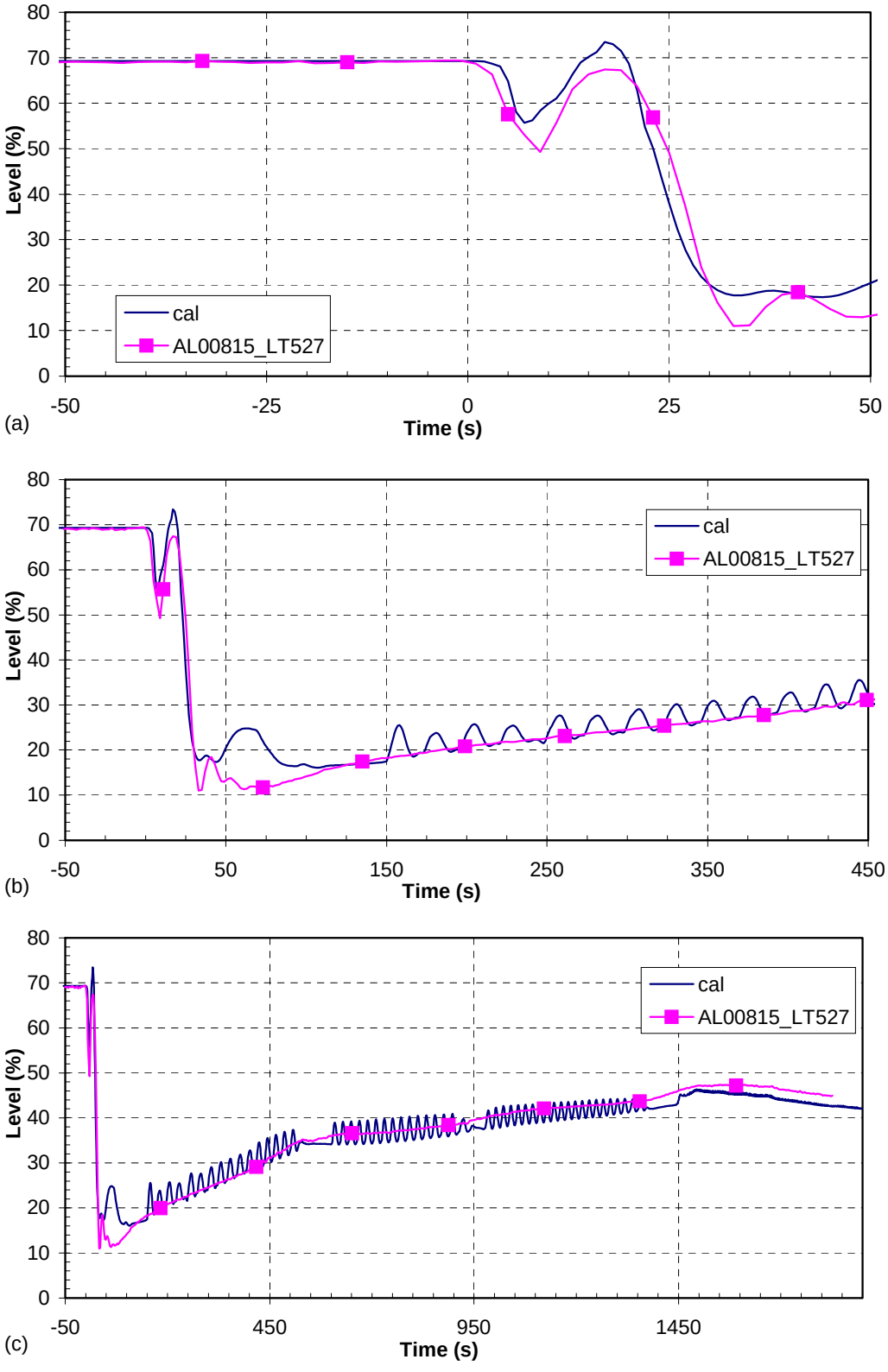


**Figure 36 SG 2 narrow range level—turbine governor valve closure with reactor trip**

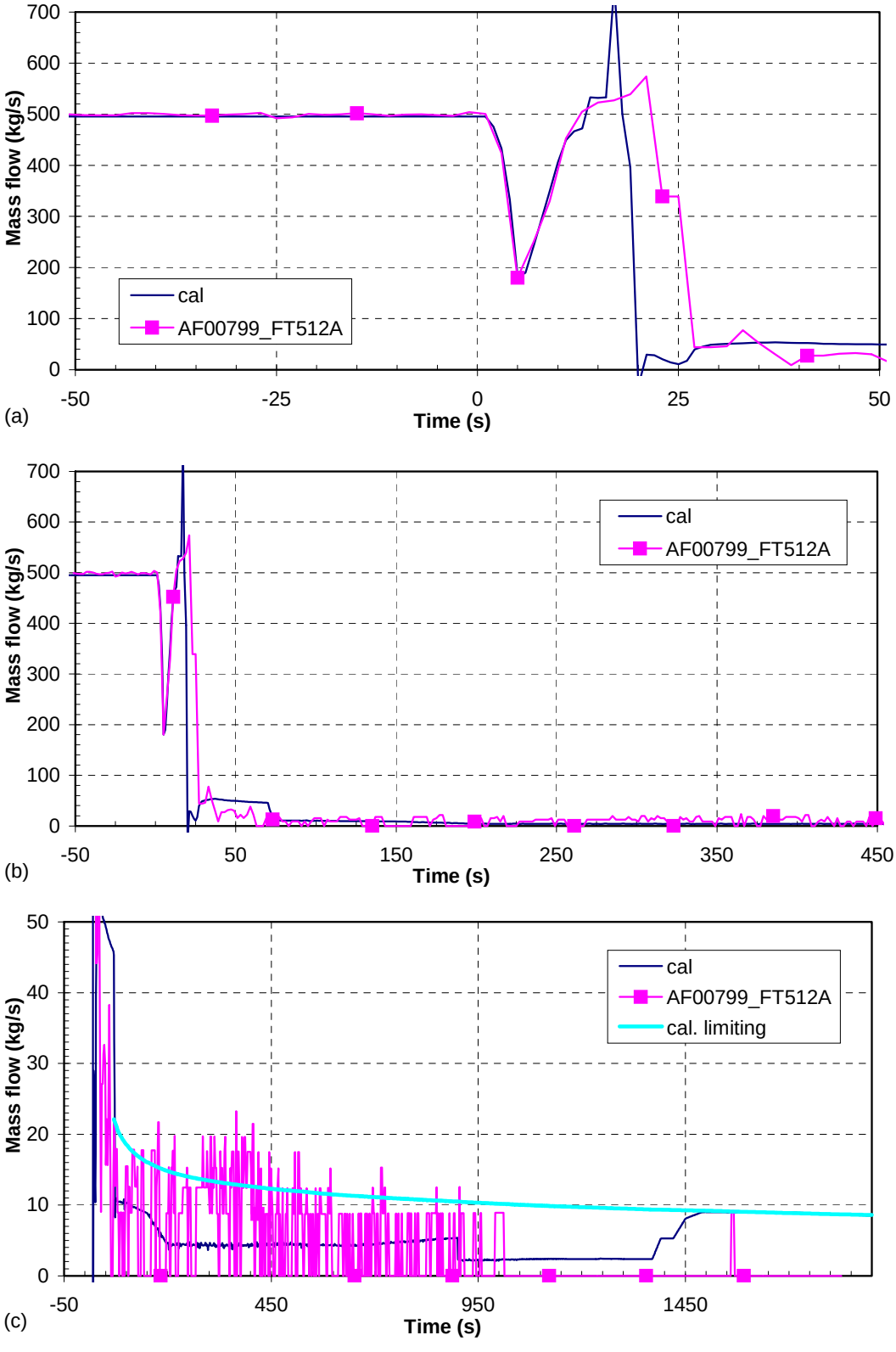


**Figure 37 Steamflow SG 1—turbine governor valve closure with reactor trip**

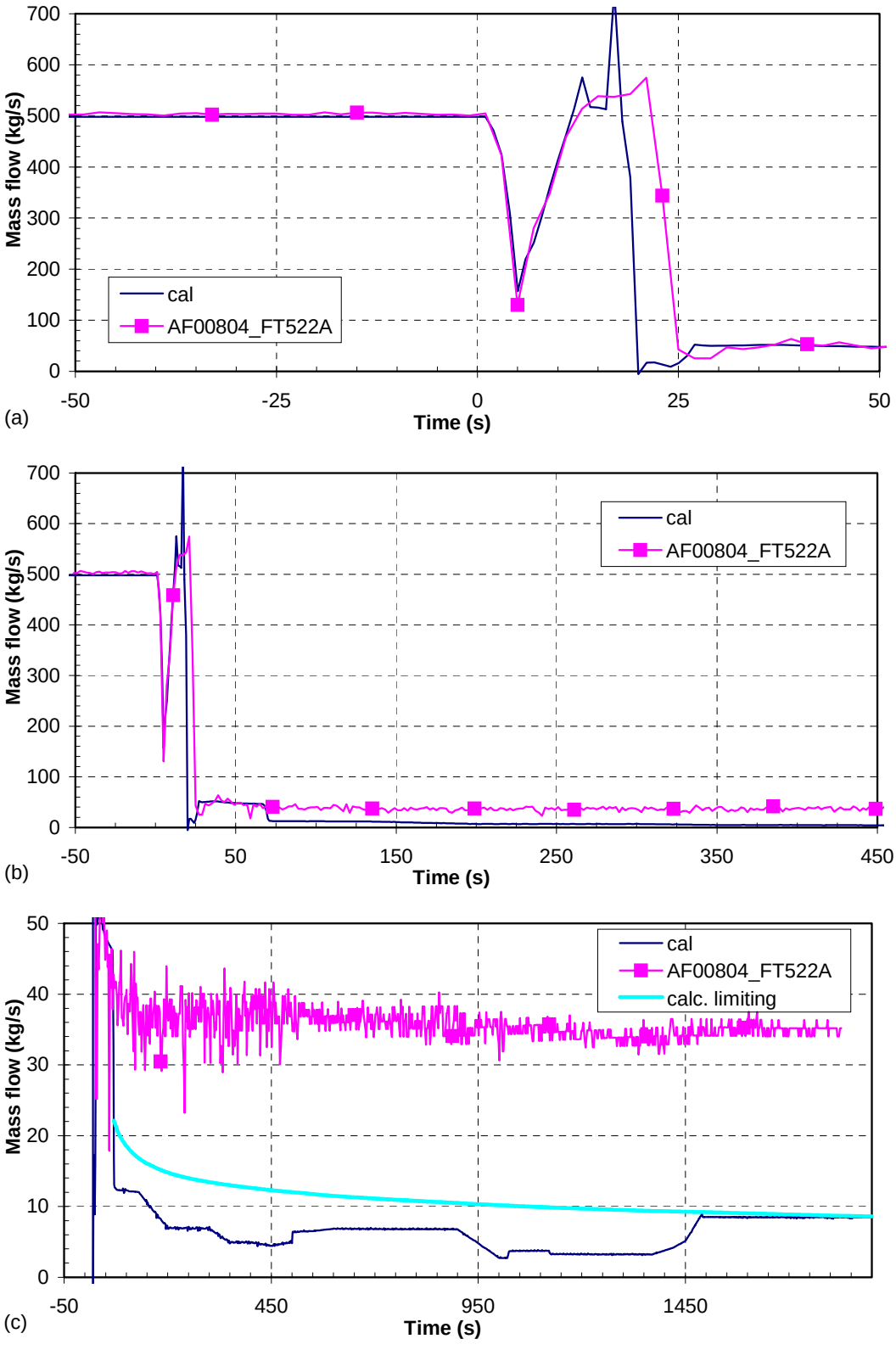


**Figure 38 Steamflow SG 2—turbine governor valve closure with reactor trip**

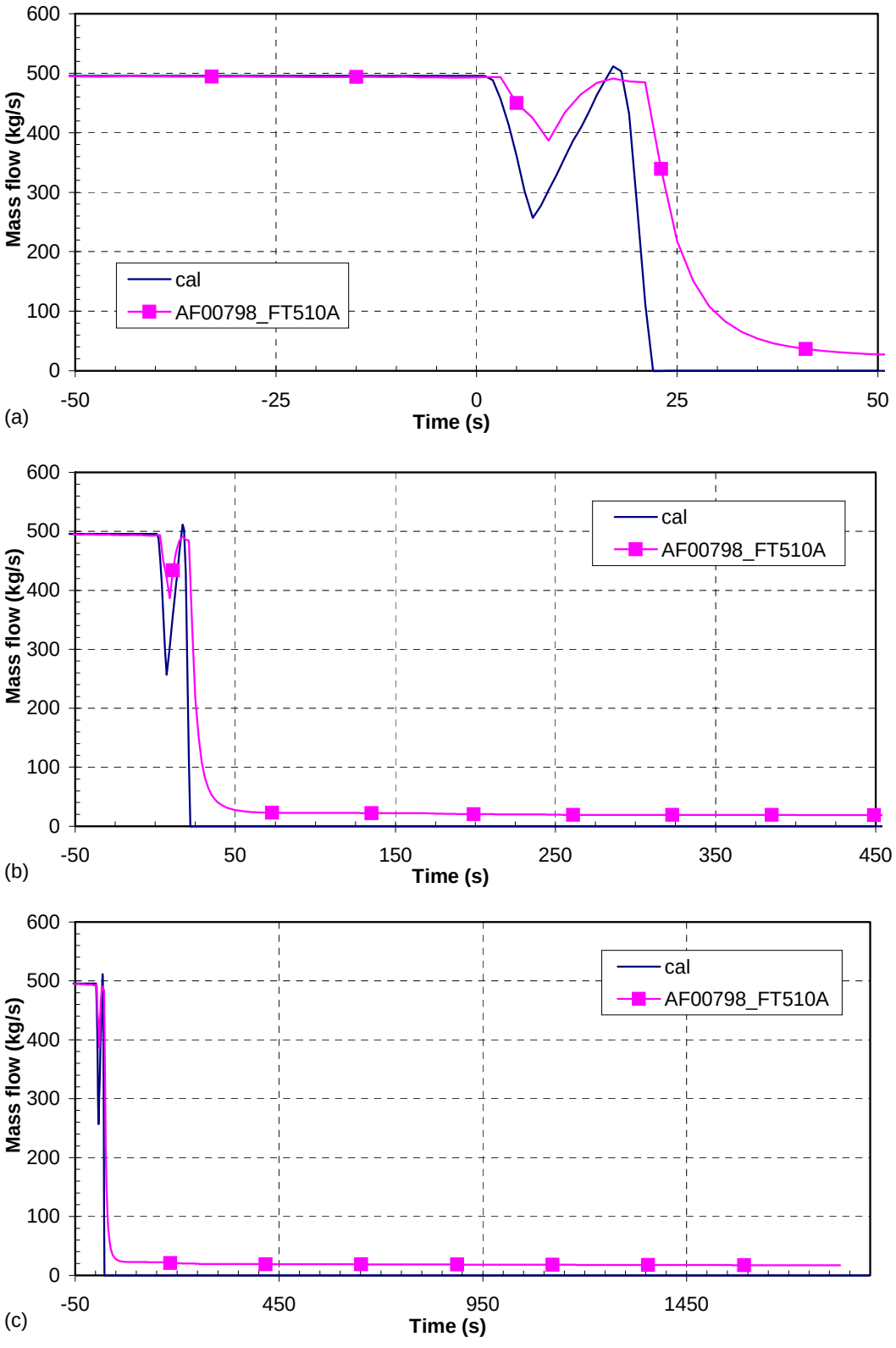


**Figure 39 Feedwater flow SG 1—turbine governor valve closure with reactor trip**

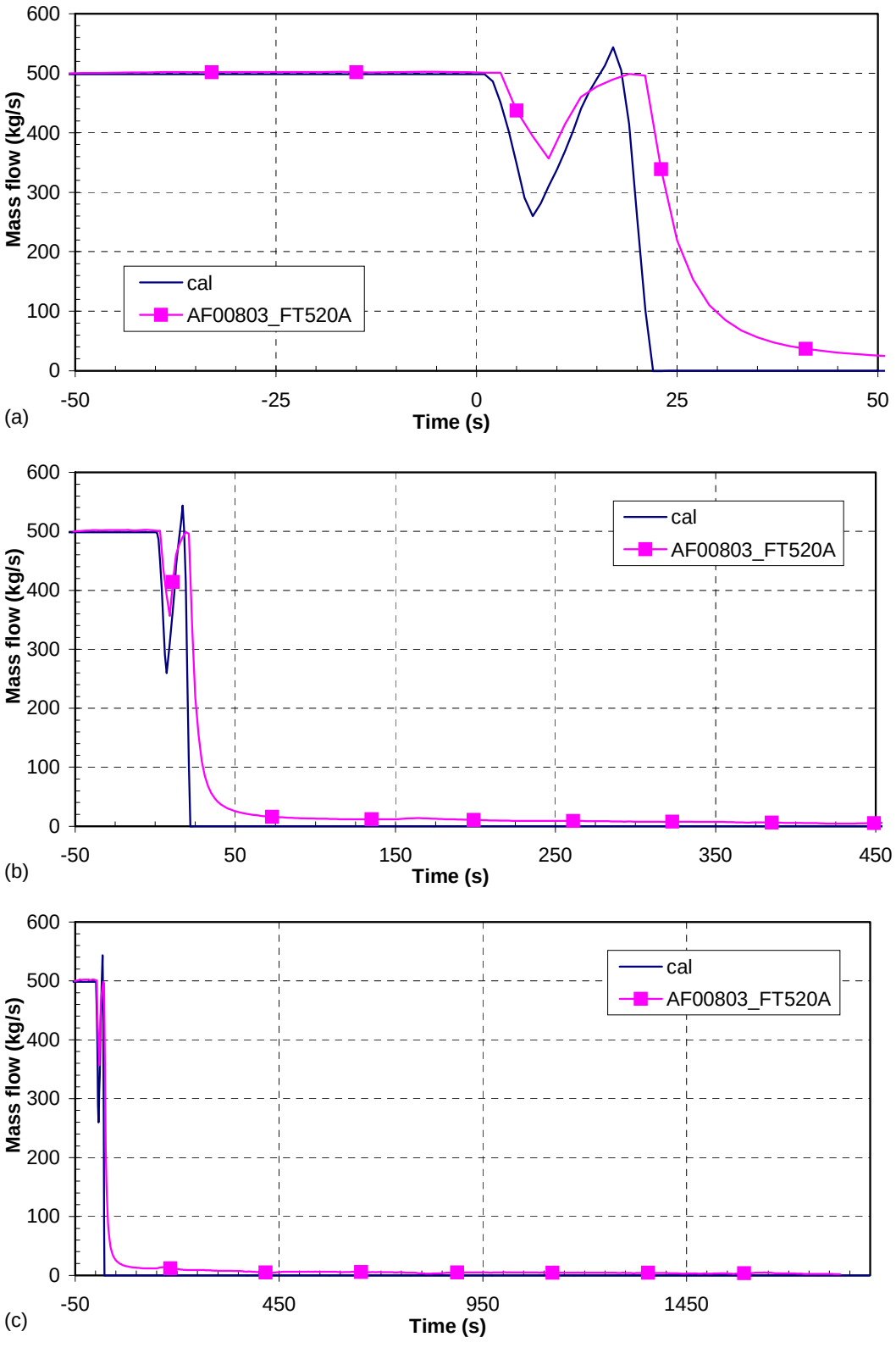


**Figure 40 Feedwater flow SG 2—turbine governor valve closure with reactor trip**

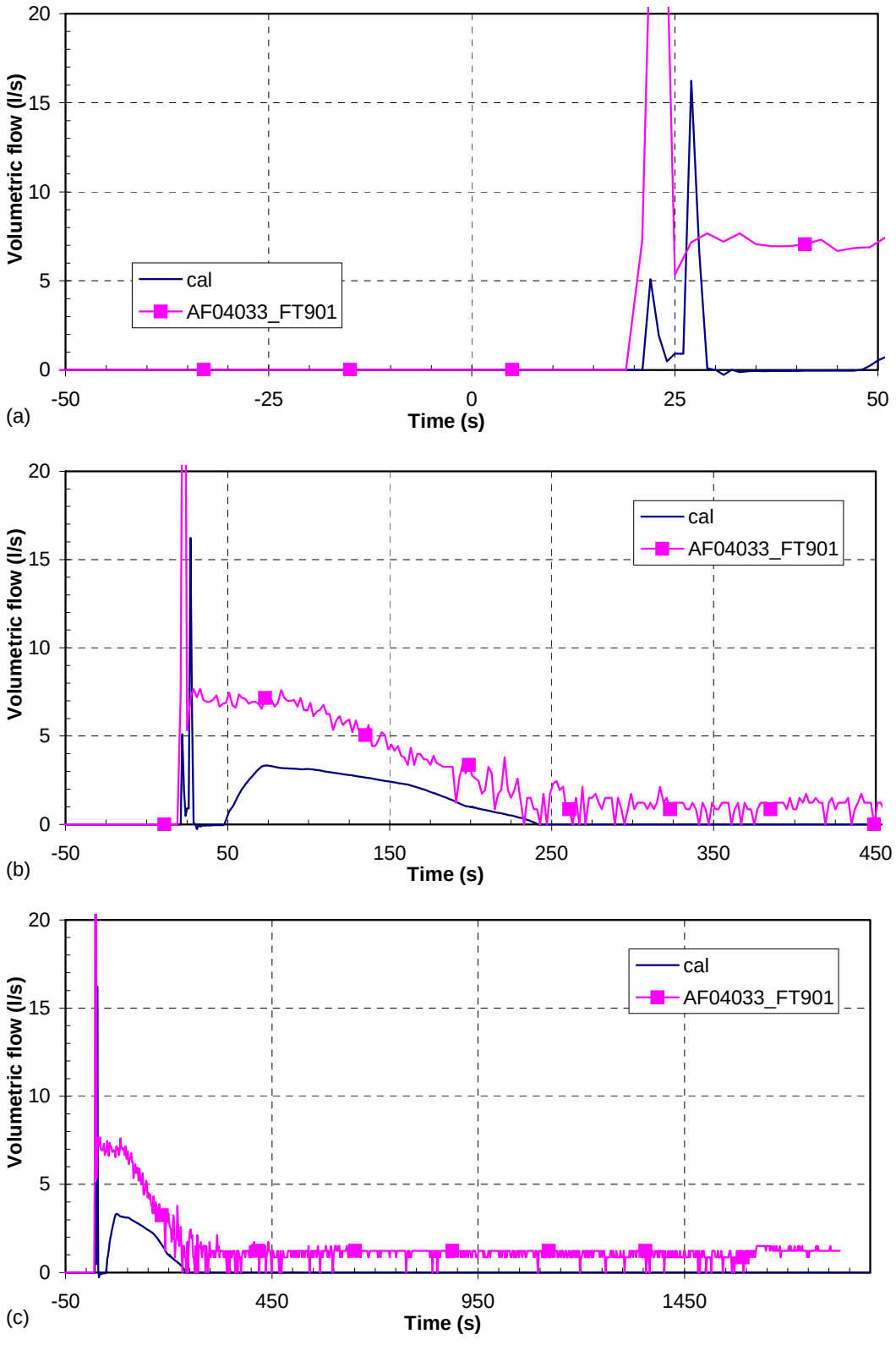


**Figure 41 SI 1 volumetric flow—turbine governor valve closure with reactor trip**

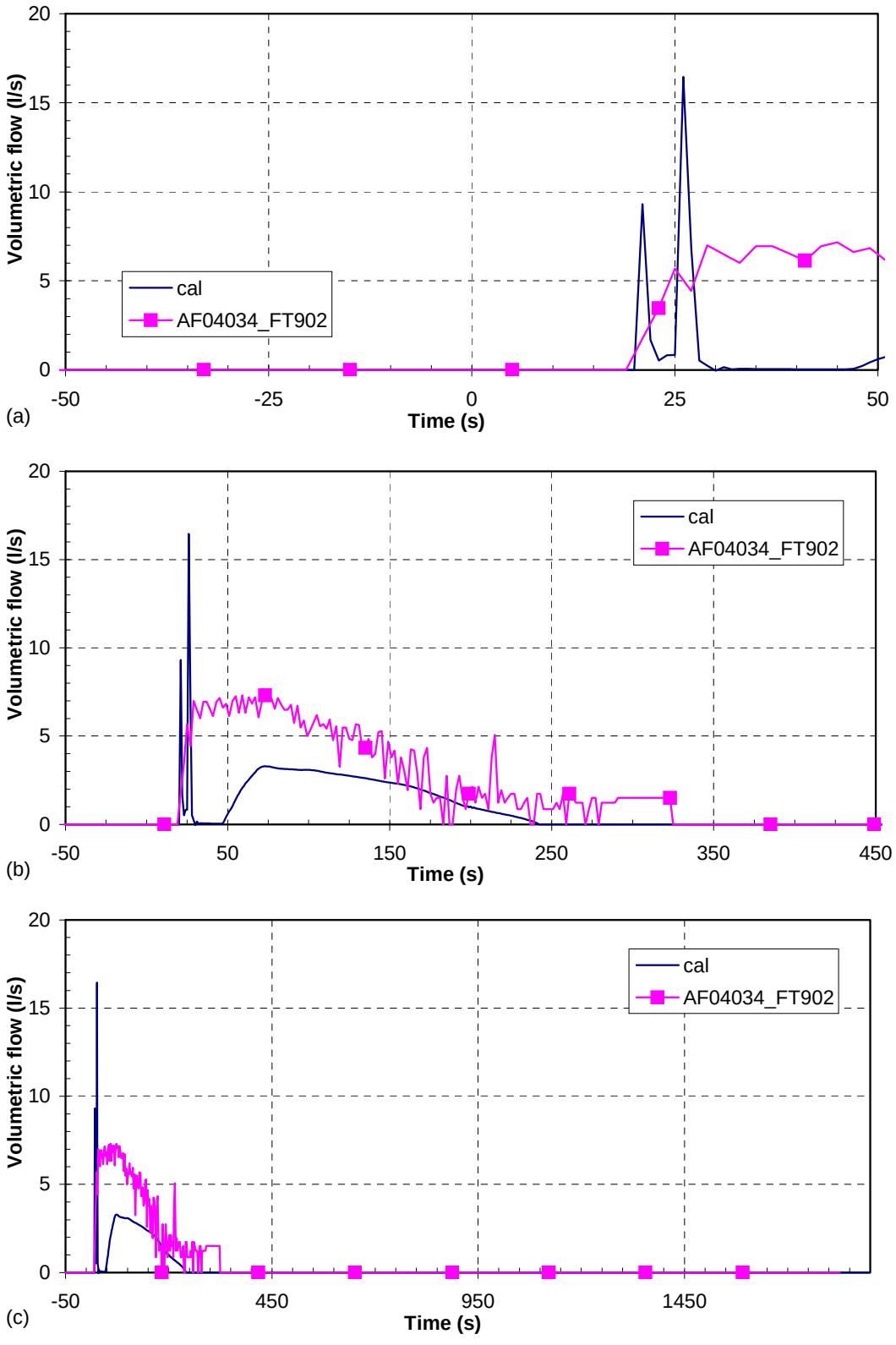


**Figure 42 SI 2 volumetric flow—turbine governor valve closure with reactor trip**

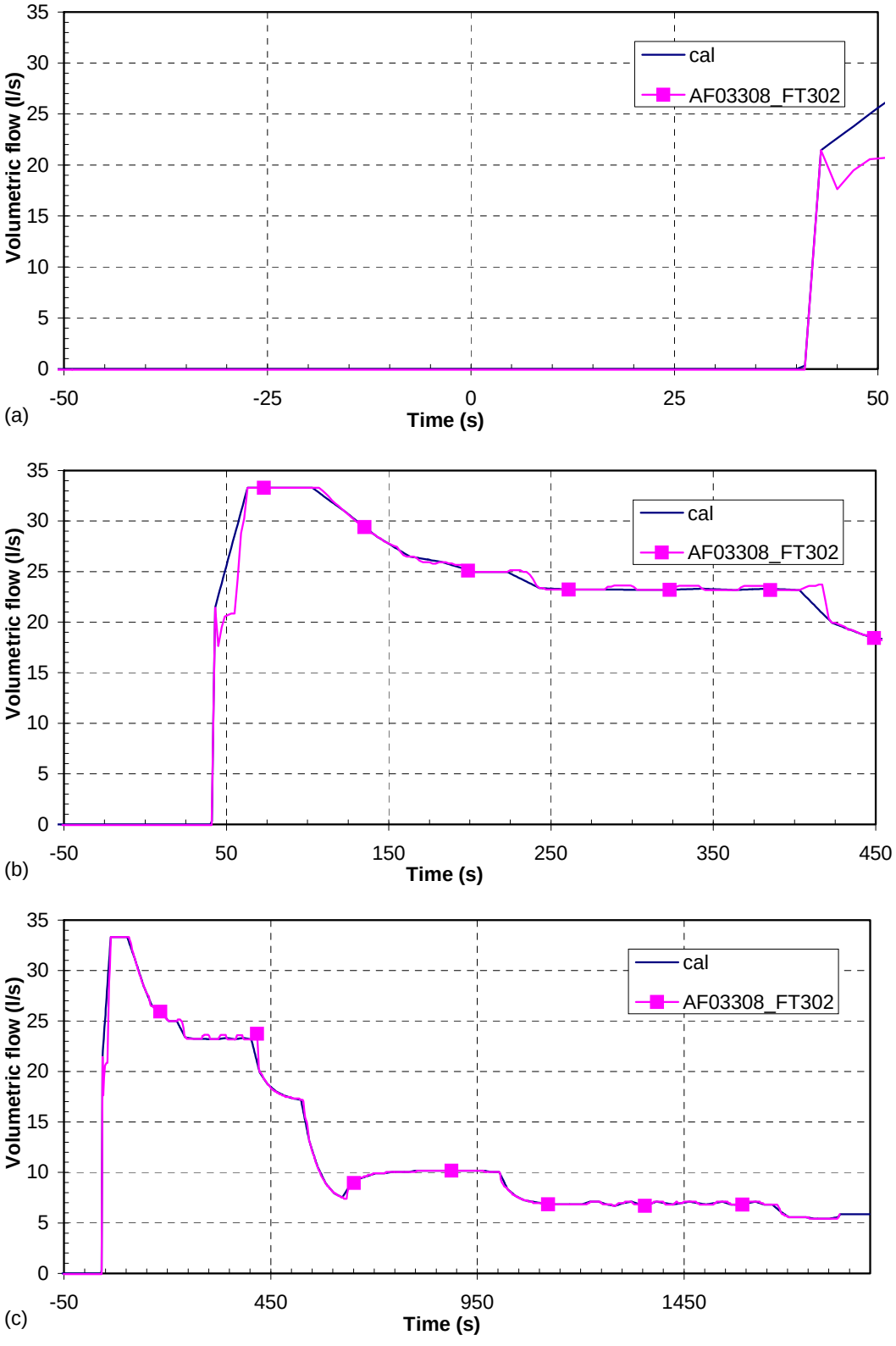


**Figure 43 AFW 1 volumetric flow—turbine governor valve closure with reactor trip**

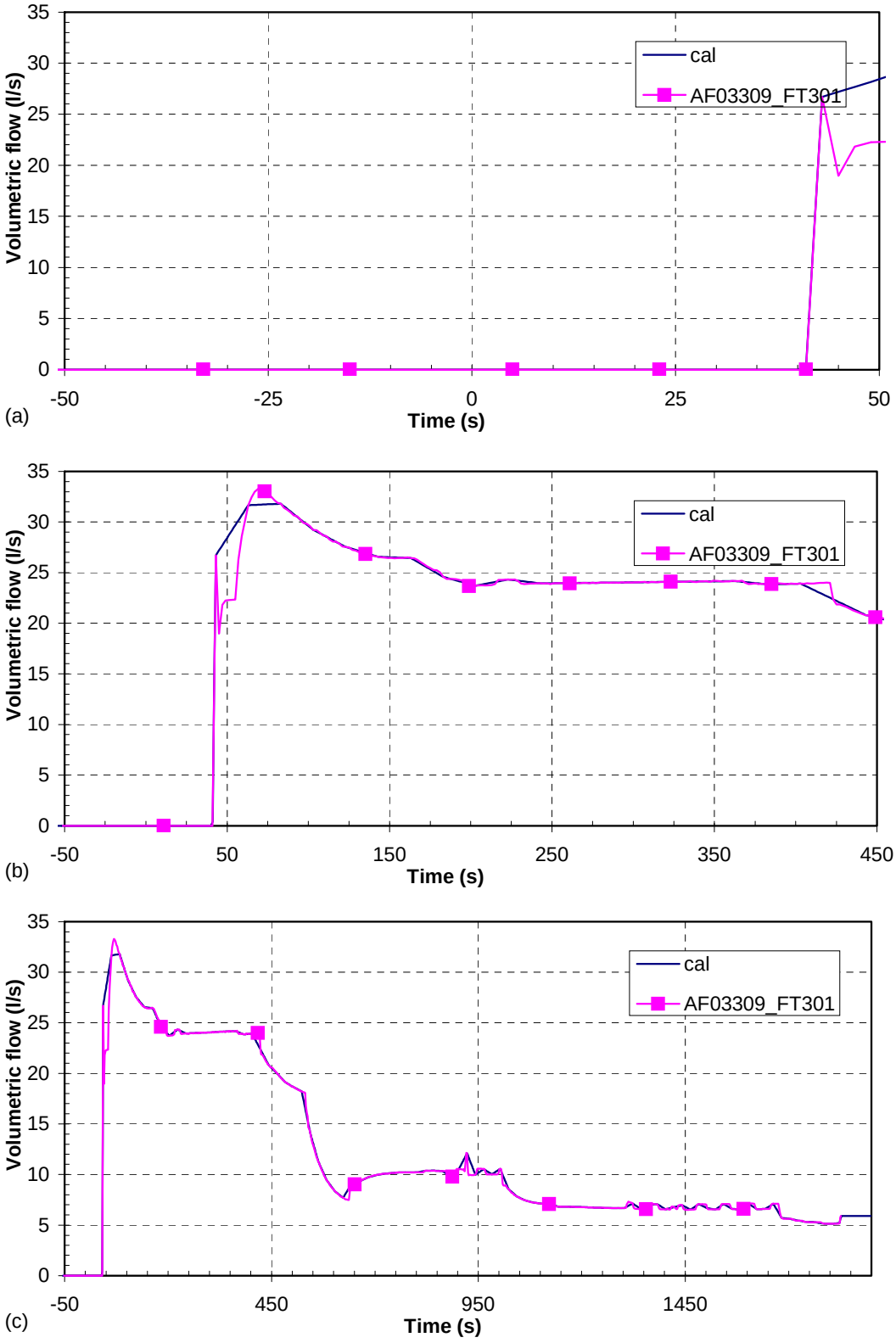


**Figure 44 AFW 2 volumetric flow—turbine governor valve closure with reactor trip**

# 6. RUN STATISTICS

The transient was calculated using a Hewlett Packard personal computer with a 1.60-gigahertz Intel Pentium M processor running Microsoft Windows XP, Professional Version 2002, Service Pack 2. Table 5 summarizes the run statistics. Note that the CPU time was shorter than that of the actual transient duration.

**Table 5 Run Statistics**

| | |
|---|---|
| Number of volumes | 469 |
| Number of time steps | 54523 |
| Transient time | 1900 s |
| CPU time | 1166.6 s |
| CPU time/Transient time | 0.61 |

# 7. CONCLUSIONS

This study evaluated the RELAP5/MOD3.3 P03 computer code against plant-measured data for the reactor trip that occurred at the Krško NPP on April 10, 2005. In addition to the code assessment, the analysis served to validate the input model for the Krško NPP, which is a two-loop Westinghouse PWR.

The event analyzed was a malfunction that occurred during a power reduction sequence while regular, periodic testing of the turbine valves was performed. The reactor trip analysis was divided into two parts. In the first part, the power was reduced from a nominal value of 100 percent to test conditions at around 91.72 percent. The first part of the analysis also simulated the testing of the turbine governor valves. The second part of the analysis simulated the turbine governor valve closure with reactor trip, as well as the associated operator actions.

A steady state of 91.72-percent power was achieved by manipulating the plant RELAP5 model. in such a way that the calculated initial conditions were close to the initial conditions at the plant. The results demonstrated that the transient very much depends on both the primary- and secondary-side injection flows. After the initial phase of the transient, the operators set the flows; therefore, it was necessary to use the plant-measured data in the calculation for charging and letdown on the primary side and the AFW on the secondary side. The analysis revealed that the long-term transient evolution is very sensitive to steamflow following a reactor trip. The calculation showed that the measured steamflow was larger than the calculated steam generated by available decay heat and as consequence measurement of steamflow after reactor trip was not reliable. Therefore, the steamflow was tuned to obtain as good a match to the measured SG pressure as possible.

In general, the analysis found that proper modeling of operator actions was needed to obtain good agreement between the calculated results and the plant-measured data. Initially, proper modeling of the governor valve closure was required to obtain the SI signal upon low steamline pressure. In the later phase, proper modeling of the filling of the primary and secondary system was important. Without modeling the operator actions which happened, close agreement between calculation and measured data would not be achieved. Finally, the calculated data may be used to supplement plant-measured data when the information is missing or the measurement is questionable.

# 8. REFERENCES


1. U.S. Nuclear Regulatory Commission, “RELAP5/MOD3.3 Code Manual,” NUREG/CR-5535, Rev. P3, Information Systems Laboratories, Inc., Nuclear Safety Analysis Division, Idaho Falls, ID. Prepared for the NRC, Washington, DC, March 2003.
2. Parzer, I., B. Mavko, and B. Krajnc, “Simulation of a Hypothetical Loss-of-Feedwater Accident in a Modernized Nuclear Power Plant,” *Journal of Mechanical Engineering*, 2003, Vol. 49, No. 9, pp. 430–444.
3. Prošek, A., I. Parzer, and B. Krajnc, “Simulation of Hypothetical Small-Break Loss-of-Coolant Accident in Modernized Nuclear Power Plant,” *Electrotechnical Review*, 2004, Vol. 71, No. 4, pp. 199–204.
4. Parzer, I., “Break Model Comparison in Different RELAP5 Versions,” *International Conference Nuclear Energy for New Europe 2003, September 8-11, 2003*, Portorož, Slovenia, Nuclear Society of Slovenia, 2003, pp. 217.1–217.8.